

Titre: Effects of internal and external flow on the vibration characteristics of anisotropic cylindrical shells
Title:

Auteurs: Aouni A. Lakis
Authors:

Date: 1977

Type: Rapport / Report

Référence: Lakis, A. A. (1977). Effects of internal and external flow on the vibration characteristics of anisotropic cylindrical shells. (Rapport technique n° EP-R-77-11). <https://publications.polymtl.ca/6154/>
Citation:

 **Document en libre accès dans PolyPublie**
Open Access document in PolyPublie

URL de PolyPublie: <https://publications.polymtl.ca/6154/>
PolyPublie URL:

Version: Version officielle de l'éditeur / Published version

Conditions d'utilisation: Tous droits réservés / All rights reserved
Terms of Use:

 **Document publié chez l'éditeur officiel**
Document issued by the official publisher

Institution: École Polytechnique de Montréal

Numéro de rapport: EP-R-77-11
Report number:

URL officiel:
Official URL:

Mention légale:
Legal notice:



DÉPARTEMENT DE GÉNIE MÉCANIQUE
SECTION DESIGN de MACHINES

EFFECTS OF INTERNAL AND EXTERNAL
FLOW ON THE VIBRATION CHARACTERISTICS
OF ANISOTROPIC CYLINDRICAL SHELLS

by

Aouni A. Lakis

NO EP 77-R-11

Février 1977

Ecole Polytechnique de Montréal

CA2PQ

UP4

77R11

Campus de l'Université
de Montréal
Case postale 6079
Succursale 'A'
Montréal, Québec
H3C 3A7

Bibliothèque

**Ecole
Polytechnique**

COTE

CA2PQ

MONTREAL

96982

UP4

77RLL



9 MARS 1977

EFFECTS OF INTERNAL AND EXTERNAL
FLOW ON THE VIBRATION CHARACTERISTICS
OF ANISOTROPIC CYLINDRICAL SHELLS

by

Aouni A. Lakis

RAPPORT TECHNIQUE NO EP 77-R-11

Département de Génie Mécanique
Ecole Polytechnique
Montréal, P.Q., Canada

Février 1977

Amc

CONTENTS

	<u>Page</u>
1. INTROUDCTION	1
2. GENERAL APPROACH	5
2.1 General theory	5
2.2 Equations of motion	6
2.3 The displacement functions	8
2.4 Determination of the mass and stiffness matrices	12
2.5 Elasticity matrix	16
2.6 Stiffness and matrices for the whole shell in vacuo	17
3. FREE VIBRATION	18
4. EFFECTS OF COMPRESSIBLE FLOW	20
4.1 Mass, stiffness and damping matrices of the moving fluid	20
5. PRESSURE FLUCTUATIONS INDUCED BY INTERNAL FLOW	25
5.1 Representation of pressure field at nodal points	26
5.2 Mean square response	27
6. METHOD OF CALCULATION AND DISCUSSION	30
7. CONCLUSION	35
ACKNOWLEDGEMENTS	36
APPENDIX I	37
APPENDIX II : References	38
APPENDIX III: Notation	41
APPENDIX IV : Figures	44

EFFECTS OF INTERNAL AND EXTERNAL
FLOW ON THE VIBRATION CHARACTERISTICS
OF ANISOTROPIC CYLINDRICAL SHELLS

Aouni A. Lakis,
Department of Mechanical Engineering,
Ecole Polytechnique,
Montreal, Que., Canada.

SUMMARY

This paper presents a general theory for the dynamic analysis of anisotropic thin cylindrical shells containing turbulent flowing fluid. The shell may be uniform or non-uniform, provided it is geometrically axially symmetric. This is a finite-element theory, using cylindrical finite elements, but the displacement functions are determined by using classical shell theory. A new solution of the wave equation of the liquid finite element leads to an expression of the fluid pressure, p , as a function of the nodal displacements of the element and three operative forces (inertia, centrifugal and Coriolis) of the moving fluid. The random pressure forces are lumped at the nodes of the finite elements. The mean square response of the displacements of the shell are obtained for a boundary-layer pressure field. Some calculations are conducted to illustrate the theory. This theory is compared with the experiments of others and agreement is found to be quite good.

1. INTRODUCTION

Thin shells appear as components in practically every type of modern industrial equipment, in aerospace, nuclear, marine and petrochemical industries. A careful study of the shells used in practical applications leads to the conclusion that they are most often anisotropic (naturally or structurally) and in many cases are anisotropic and laminar. The need is evident for a theory which can be used for the dynamical analysis of any kind of anisotropic circular cylindrical shell subjected to various boundary conditions.

Such shells are commonly used to contain or convey fluids, and this, to a certain extent, determines the classes of problems in which interest is focused. Thus, in addition to the determination of the vibration characteristics of the shells in vacuo, it is also of considerable interest to determine the dynamical characteristics of shells containing either stationary or flowing fluid.

There are many ways in which the presence of the fluid may influence the dynamics of the shell. If the shell contains a stationary gas at low pressure, then the vibration of the shell differs only slightly from that of the same shell in vacuo. This is not the case, however, if the shell is substantially pressurized by the enclosed fluid, as this entails additional strain energy in the shell. Moreover, if the fluid is compressible, the compressibility of the fluid alters the effective stiffness of the system. Also, if the density of the enclosed fluid is relatively high, as



is the case with liquids, then the fluid exerts considerable inertial loading on the shell, and this results in diminishing the resonant frequencies significantly.

Coupling between the fluid and the shell can manifest itself in several other ways, In the case of shells partially filled with liquid, free-surface motions may be coupled to the shell motions. This is of particular interest in liquid-propelled rockets; in cases of proximity or coincidence of the natural frequencies of the free surface motion and that of the shell, large oscillations may develop in the propellant tanks and are normally referred to as sloshing. Nonlinear coupling may also induce sloshing; in this case subharmonic excitation of free-surface modes is involved.

Other effects of coupled fluid-shell motions occur when the fluid is flowing. Depending upon the boundary conditions, if the flow velocities are large, buckling or oscillatory flexural instabilities are possible.

Similarly, in considering the response of cylindrical shells, considerable interest exists in the case where the excitation is transmitted through, or arises from, the contained fluid. This could take the form of pressure waves transmitted through the fluid; or, if the fluid is flowing, the excitation could arise from gross pressure perturbations due to disturbances in the flow, or from boundary-layer perturbations. It is known that vibration caused by these pressure fluctuations may, in certain circumstances, cause fatigue failures of the structures involved.

Several methods have been developed for the dynamical analysis of shells. Of these the most versatile have proved to be Rayleigh-Ritz methods [1 - 2]*, Stodola-type iteration methods [3], finite-difference method [4] and finite-element methods [5 - 10]. All these methods and their variants have their advantages and disadvantages. One of the criteria of success of a method may be considered to be its capability of yielding the high, as well as the low, characteristic frequencies and modal shapes with comparable high accuracy. This requirement is not really met by the finite-difference and Stodola-type methods [4]. The Rayleigh-Ritz and finite-element methods, on the other hand, are satisfactory from this point of view; furthermore, because they lead to a symmetric eigenvalue problem, they are easily amenable to solution by digital computer, which is great advantage. The finite-element method has added advantages in terms of ease of formulation, and because numerical convergence is not as sensitive to particular sets of boundary conditions as is the case with the Rayleigh-Ritz method [11].

Here we shall present a finite-element type of theory which is capable of giving highly accurate prediction of the free vibration characteristics of cylindrical shells, and their response when subjected to a random pressure field. The theory can also deal with shells partially filled with liquid.

The analysis is based on a recently developed method for the case of isotropic cylindrical shells [12]. It is a hybrid theory based on the finite-element method, with the displacement functions determined by exact

* References are given in Appendix II.

solution of the equations of equilibrium of a thin cylindrical shell instead of the more usual polynomial displacement functions. The finite elements are cylindrical frusta; thus a given non-uniform shell is first subdivided into its component uniform cylindrical segments and then, generally each segment is similarly subdivided into a number of cylindrical finite elements.

The theory for predicting the response of anisotropic cylindrical shells due to random pressure fields is developed in reference [13]. The continuous pressure field is transformed to a discrete set of forces; then the cross-correlation spectral density and the mean square values of the displacement of the shell are expressed in terms of correlation functions of the boundary-layer pressure fields.

Here the dynamics of an anisotropic cylindrical shell and its response will be considered, with the following aims: (i) to extend the theory of [12] to cases where the shells are anisotropic and especially for the case of shells consisting of an arbitrary number of orthotropic layers; (ii) to develop a theory accounting for the effects of compressible flow on the free vibration characteristics of a thin, cylindrical shells; (iii) to use the theory of [13] to predict the response of such shells to a pressure field arising from the turbulent boundary-layer of internal flow, to the point of predicting R.M.S. amplitudes of vibration.

This generalized theory will be more directly pertinent to engineering applications, since in nearly all practical cases the shells are often ani-

sotropic; e.g., heat exchangers and liquid metal cooled channels used in the nuclear industry. A number of assumptions are made during the course of the investigation; a compendium of these assumptions and the limitations of the theory will be given in the text.

2. GENERAL APPROACH

2.1 General theory

A given shell is subdivided into a number of finite elements, each being defined by the two nodes, i and j , and the corresponding nodal circle boundaries (Fig. 1). Then, the displacement functions may be defined by

$$\left[U(x, \phi), W(x, \phi), V(x, \phi) \right]^T = \left[N \right] \left[\delta_i, \delta_j \right]^T \quad (1)$$

where $\{\delta_i\}$ and $\{\delta_j\}$ represent the nodal displacements, and the elements of $\left[N \right]$ are in general functions of position and the shell's anisotropy.

It is noted that the finite-element method yields useful results provided that the displacement functions chosen represent adequately the true displacements; accordingly, the displacement functions should satisfy the convergence criterion of the finite-element method stating that strains within the element should be zero when the nodal displacements are generated by rigid-body motions. To this end, we shall employ the equations of thin cylindrical shells to obtain the displacement functions, instead of using the more common arbitrary polynomial forms.

Sander's theory [14] for thin cylindrical shells is used for the determination of these displacement functions. This shell theory which is based on Love's first approximation was preferred, for the following reason: in Sander's theory all strains vanish for small rigid body motions, which is not true for Love's or Timoshenko's theories, for instance. By using such displacement functions, we automatically satisfy the convergence criterion of the finite-element method previously stated.

2.2 Equations of Motion

Using Love's first approximation, we obtain the following elasticity relationships between the stress-resultant and the deformations of the middle surface for the general case of a multi-layer anisotropic shell

$$\left\{ \begin{array}{c} N_x \\ N_\phi \\ \bar{N}_{x\phi} \\ M_x \\ M_\phi \\ \bar{M}_{x\phi} \end{array} \right\} = [P] \{ \epsilon \}, \quad (2) \quad [P] = \begin{bmatrix} p_{11} & p_{12} & 0 & p_{14} & p_{15} & 0 \\ p_{21} & p_{22} & 0 & p_{24} & p_{25} & 0 \\ 0 & 0 & p_{33} & 0 & 0 & p_{36} \\ p_{41} & p_{42} & 0 & p_{44} & p_{45} & 0 \\ p_{51} & p_{52} & 0 & p_{54} & p_{55} & 0 \\ 0 & 0 & p_{63} & 0 & 0 & p_{66} \end{bmatrix}, \quad (3)$$

the elements p_{ij} of the elasticity matrix $[P]$ characterize the shell's anisotropy which depends on the mechanical properties of the material of the structure.

The strain vector $\{\epsilon\}$ is the modified strain-displacement relations of Sanders [14] and is given by

$$\{\epsilon\} = \begin{Bmatrix} \epsilon_x \\ \epsilon_\phi \\ 2\epsilon_{x\phi} \\ \kappa_x \\ \kappa_\phi \\ 2\bar{\kappa}_{x\phi} \end{Bmatrix} = \begin{Bmatrix} \partial u/\partial x \\ (1/r) (\partial V/\partial \phi) + (W/r) \\ \partial V/\partial x + (1/r) (\partial U/\partial \phi) \\ -\partial^2 W/\partial x^2 \\ -(1/r^2) [(\partial^2 W/\partial \phi^2) - (\partial V/\partial \phi)] \\ -(2/r) (\partial^2 W/\partial x \partial \phi) + (3/2r) (\partial V/\partial x) - (1/2r^2) (\partial U/\partial \phi) \end{Bmatrix} \quad (4)$$

Upon substituting equations (2) - (4) into Sanders shell equations of motion, the author obtains the equations of equilibrium in terms of elements p_{ij} of $[P]$ and in terms of U , V and W , namely

$$\begin{aligned} & p_{11} (\partial^2 U/\partial x^2) + (1/r)p_{12} (\partial W/\partial x) - p_{14} (\partial^3 W/\partial x^3) + [(1/r) (p_{12} + p_{33}) + (1/r^2)(p_{15} + p_{36}) - (3/4r^3) p_{66}] \cdot \\ & \cdot (\partial^2 V/\partial \phi \partial x) + (1/r^2) [p_{33} - (1/r) p_{36} + (1/4r^2) p_{66}] (\partial^2 U/\partial \phi^2) - (1/r^2) [p_{15} + 2p_{36} - \\ & - (1/r)p_{66}] (\partial^3 W/\partial x \partial \phi^2) = 0, \\ & (1/r) [p_{33} + p_{21} + (1/r) p_{36} + (1/r) p_{51} - (3/4r^2) p_{66}] (\partial^2 U/\partial \phi \partial x) + (1/r^2) [p_{22} + (1/r^2) p_{55} + \\ & + (2/r) p_{25}] (\partial^2 V/\partial \phi^2) + [p_{33} + (3/r) p_{36} + (9/4r^2) p_{66}] (\partial^2 V/\partial x^2) + [p_{22} + (1/r) p_{52}] (1/r^2) \cdot \\ & \cdot (\partial W/\partial \phi) - (1/r^3) [p_{25} + (1/r) p_{55}] (\partial^3 W/\partial \phi^3) - (1/r) [2p_{36} + p_{24} + (3/r) p_{66} + (1/r) p_{54}] \cdot \\ & \cdot (\partial^3 W/\partial \phi \partial x^2) = 0, \\ & -(1/r)p_{21} (\partial U/\partial x) - (1/r^2) [p_{22} + (1/r) p_{25}] (\partial V/\partial \phi) - (1/r^2) p_{22} W + p_{41} (\partial^3 U/\partial x^3) + (1/r^2) [p_{51} + \\ & + 2p_{63} - (1/r)p_{66}] (\partial^3 U/\partial x \partial \phi^2) + (1/r^3) [p_{52} + (1/r) p_{55}] (\partial^3 V/\partial \phi^3) + (1/r) [p_{42} + 2p_{63} + \\ & + (1/r)p_{45} + (3/r)p_{66}] (\partial^3 V/\partial \phi \partial x^2) + (2/r^3) p_{25} (\partial^2 W/\partial \phi^2) - (1/r^4) p_{55} (\partial^4 W/\partial \phi^4) + (2/r) p_{24} \cdot \\ & \cdot (\partial^2 W/\partial x^2) - p_{44} (\partial^4 W/\partial x^4) - (1/r^2) (2p_{45} + 4p_{66}) (\partial^4 W/\partial x^2 \partial \phi^2) = 0 \end{aligned} \quad (5)$$

Here U , V and W are, respectively, the axial, circumferential and radial displacements of the middle surface of the shell, and r its mean radius (Fig. 1). The solution of these equations will give the displacement functions.

2.3 The displacement functions

In the continuum, we express U , V and W of the middle surface of the shell by

$$\begin{Bmatrix} U(x, \phi) \\ W(x, \phi) \\ V(x, \phi) \end{Bmatrix} = \sum_{n=0}^{\infty} \begin{bmatrix} \cos n\phi & 0 & 0 \\ 0 & \cos n\phi & 0 \\ 0 & 0 & \sin n\phi \end{bmatrix} \begin{Bmatrix} u_n(x) \\ w_n(x) \\ v_n(x) \end{Bmatrix} = \sum_{n=0}^{\infty} \{T\} \begin{Bmatrix} u_n(x) \\ w_n(x) \\ v_n(x) \end{Bmatrix} \quad (6)$$

where n is the circumferential wave-number. By substituting equation (6) into equation (5) and letting

$$u_n(x) = A e^{\lambda x/r}, \quad v_n(x) = B e^{\lambda x/r}, \quad w_n(x) = C e^{\lambda x/r}, \quad (7)$$

we obtain three simultaneous ordinary linear equations in A , b , C of the form

$$[H] \begin{Bmatrix} A \\ B \\ C \end{Bmatrix} = \{0\}. \quad (8)$$

For non-trivial solution, the determinant of $[H]$ must vanish, leading to the following characteristic equation

$$h_8 \lambda^8 - h_6 \lambda^6 + h_4 \lambda^4 - h_2 \lambda^2 + h_0 = 0, \quad (9)$$

where

$$h_8 = (h_9/r^2) (p_{11} p_{44} - p_{14}^2),$$

$$h_6 = (n^2/r^2) \left[h_9 (h_1 p_{44} + 2p_{11} p_{45} + 4p_{11} p_{66} - 2h_5 r p_{14}) + h_7 (p_{11} p_{44} - p_{14}^2) - r^2 h_{11}^2 p_{11} - h_3^2 p_{44} + 2r h_3 h_{11} p_{14} \right] + (2/r) h_9 (p_{11} p_{24} - p_{14} p_{12}),$$

$$h_4 = (n^4/r^2) \left[h_1 h_7 p_{44} + h_9 p_{11} p_{55} + (2p_{45} + 4p_{66}) (h_1 h_9 + h_7 p_{11} - h_3^2) + (p_{25} + (1/r) p_{55}) \cdot (2h_3 p_{14} - 2h_{11} p_{11} r) + h_{11} r^2 (2h_3 h_5 - h_1 h_{11}) - r h_5 (2h_7 p_{14} + r h_5 h_9) \right] + (n^2/r) \cdot \left[2(p_{25} + r p_{22}) ((h_3/r) p_{14} - h_{11} p_{11}) - 2p_{12} (h_5 h_9 r + h_7 p_{14} - h_3 h_{11} r) - 2p_{24} (h_3^2 - h_1 h_9 - h_7 p_{11}) + 2h_9 p_{11} p_{25} \right] + h_9 (p_{11} p_{22} - p_{12}^2),$$

$$h_2 = (n^6/r^2) \left[h_1 h_7 (2p_{45} + 4p_{66}) + p_{55} (h_1 h_9 + h_7 p_{11} - h_3^2) - r^2 h_5^2 h_7 + (p_{25} + (1/r) p_{55}) \cdot (-2r h_1 h_{11} + 2r h_3 h_5 - p_{11} p_{25} - (1/r) p_{11} p_{55}) \right] + (n^4/r) \left[2h_1 h_7 p_{24} + 2p_{25} (h_1 h_9 + h_7 p_{11} - h_3^2) - 2p_{12} (r h_5 h_7 - h_3 p_{25} - (h_3/r) p_{55}) - 2(p_{25} + r p_{22}) (h_1 h_{11} + (1/r) p_{11} p_{25} + (1/r^2) p_{11} p_{55} - h_3 h_5) \right] + n^2 \left[p_{22} (h_1 h_9 + h_7 p_{11} - h_3^2) - (1/r) (p_{25} + r p_{22}) ((1/r) p_{11} p_{25} + p_{11} p_{25} - 2h_3 p_{12}) - h_7 p_{12}^2 \right],$$

$$h_0 = n^4 h_1 h_7 \left[p_{22} + (2/r) n^2 p_{25} + (n^4/r^2) p_{55} \right] - n^2 h_1 \left[(n^3/r) (p_{25} + (1/r) p_{55}) + (n/r) (p_{25} + r p_{22}) \right]^2$$

and the parameters h_i , $i=1, 3, 5, 7, 9, 11$ are given by

$$\begin{aligned} h_1 &= p_{33} - (1/r) p_{36} + (1/4r^2) p_{66}, & h_3 &= p_{12} + p_{33} + (1/r) (p_{15} + p_{36}) - (3/4r^2) p_{66}, \\ h_5 &= (1/r) (p_{15} + 2p_{36} - (1/r) p_{66}), & h_7 &= p_{22} + (1/r^2) p_{55} + (2/r) p_{25}, \\ h_9 &= p_{33} + (3/r) p_{36} + (9/4r^2) p_{66}, & h_{11} &= (1/r) \left[2p_{36} + p_{24} + (3/r) p_{66} + (1/r) p_{54} \right]. \end{aligned} \quad (10)$$

This characteristic equation for anisotropic cylindrical shells which is a quartic in λ^2 , has the same general form as equation (5) of [12] for isotropic one. The eight roots λ_i may therefore be written as follows

$$\begin{aligned}\lambda_1 &= -\kappa_1 + i\mu_1, & \lambda_2 &= -\kappa_1 - i\mu_1, & \lambda_3 &= -\kappa_2 + i\mu_2, & \lambda_4 &= -\kappa_2 - i\mu_2, \\ \lambda_5 &= \kappa_1 + i\mu_1, & \lambda_6 &= \kappa_1 - i\mu_1, & \lambda_7 &= \kappa_2 + i\mu_2, & \lambda_8 &= \kappa_2 - i\mu_2.\end{aligned}\quad (11)$$

where κ_j and μ_j are real. Each root, λ_j , yields a solution of equation (5), the complete solution being obtained by the sum of all eight with the constants A_j , B_j and C_j , $j = 1, 2, \dots, 8$.

For every j , the three constants A_j , B_j and C_j are related among each other by the linear equations (8), so that u_n , v_n and w_n may be expressed in terms of only eight constants. To this end, we let

$$A_j = \alpha_j C_j, \quad B_j = \beta_j C_j, \quad (12)$$

where α_j and β_j , for $j = 1$ and 3 , may be expressed as follows

$$\alpha_1 = \bar{\alpha}_1 + i\bar{\alpha}_2, \quad \alpha_3 = \bar{\alpha}_3 + i\bar{\alpha}_4, \quad \beta_1 = \bar{\beta}_1 + i\bar{\beta}_2, \quad \beta_3 = \bar{\beta}_3 + i\bar{\beta}_4 \quad (13)$$

The real and imaginary parts of α_j , β_j , $j = 1$ and 3 , may be obtained from the following relationships

$$\begin{bmatrix} a_{11} & a_{12} \\ a_{21} & a_{22} \end{bmatrix} \begin{Bmatrix} \alpha_j \\ \beta_j \end{Bmatrix} = \begin{Bmatrix} -a_{13} \\ -a_{23} \end{Bmatrix} \quad (14)$$

where

$$\begin{aligned}a_{11} &= n^2 h_{11} - \lambda_j^2 p_{11}, & a_{12} &= -n\lambda_j h_3, & a_{13} &= -\lambda_j(n^2 h_5 + p_{12}) + (1/r)\lambda_j^3 p_{14}, \\ a_{21} &= a_{12}, & a_{22} &= -n^2 h_7 + \lambda_j^2 h_9, & a_{23} &= -(n/r)(1 + n^2) p_{25} - np_{22} \\ & & & & & - (n^3/r^2) p_{55} + n\lambda_j^2 h_{11}.\end{aligned}$$

By inspecting the coefficients of equations (8), the other α_j , β_j can be given by

$$\begin{aligned}
 \alpha_2 &= \bar{\alpha}_1 - i \bar{\alpha}_2 & \alpha_5 &= \bar{\alpha}_5 + i \bar{\alpha}_6 = -\alpha_2 & \beta_5 &= \bar{\beta}_5 + i \bar{\beta}_6 = \beta_2 \\
 \alpha_4 &= \bar{\alpha}_3 - i \bar{\alpha}_4 & \alpha_6 &= \bar{\alpha}_5 - i \bar{\alpha}_6 = -\alpha_1 & \beta_6 &= \bar{\beta}_5 - i \bar{\beta}_6 = \beta_1 \\
 \beta_2 &= \bar{\beta}_1 - i \bar{\beta}_2 & \alpha_7 &= \bar{\alpha}_7 + i \bar{\alpha}_8 = -\alpha_4 & \beta_7 &= \bar{\beta}_7 + i \bar{\beta}_8 = \beta_4 \\
 \beta_4 &= \bar{\beta}_3 - i \bar{\beta}_4 & \alpha_8 &= \bar{\alpha}_7 - i \bar{\alpha}_8 = -\alpha_3 & \beta_8 &= \bar{\beta}_7 - i \bar{\beta}_8 = \beta_3 . \quad (15)
 \end{aligned}$$

Upon substituting the relations (12)-(15) into equation (7) and thence into equations (6) we obtain expressions for the displacement functions in terms of eight constants \bar{C}_j . These expressions may be written as

$$\begin{Bmatrix} U(x, \phi) \\ W(x, \phi) \\ V(x, \phi) \end{Bmatrix} = \sum_{n=0}^{\infty} [T][R] \{\bar{C}\} ; \quad (16)$$

where $[R]$ is given in appendix I and $\{\bar{C}\} = [\bar{C}_1 \dots \bar{C}_8]^T$. The eight \bar{C}_j are the only free constant which must be determined from eight boundary conditions, four at each edge of the finite element. The nodal displacements (Fig. 1) at nodes i , ($x = 0$) and j , ($x = \ell$) are defined by

$$\begin{Bmatrix} \delta_i \\ \delta_j \end{Bmatrix} = \{u_{ni}, w_{ni}, (dw_n/dx)_i, v_{ni}, u_{nj}, w_{nj}, (dw_n/dx)_j, v_{nj}\}^T = [A] \{\bar{C}\} , \quad (17)$$

where $[A]$ is given in appendix I, its element being determined from those of $[R]$. Finally, combining equations (16) and (17), we obtain

$$\begin{Bmatrix} U(x, \phi) \\ W(x, \phi) \\ V(x, \phi) \end{Bmatrix} = \sum_{n=0}^{\infty} [T] [R] [A]^{-1} \begin{Bmatrix} \delta_i \\ \delta_j \end{Bmatrix} = \sum_{n=0}^{\infty} [N] \begin{Bmatrix} \delta_i \\ \delta_j \end{Bmatrix} \quad (18)$$

This equation defines the displacement functions in terms of $n\phi$, x , the elements p_{ij} of $[P]$ and the nodal displacements $\begin{Bmatrix} \delta_i \\ \delta_j \end{Bmatrix}$.

2.4 Determination of the Mass and Stiffness Matrices

Substituting equations (18) into equations (4) we obtain the strain vector $\{\epsilon\}$ in terms of $\{\delta_i\}$ and $\{\delta_j\}$ as follows:

$$\{\epsilon\} = \sum_{n=0}^{\infty} \begin{bmatrix} T & 0 \\ 0 & T \end{bmatrix} [Q] [A]^{-1} \begin{Bmatrix} \delta_i \\ \delta_j \end{Bmatrix} = \sum_{n=0}^{\infty} [B] \begin{Bmatrix} \delta_i \\ \delta_j \end{Bmatrix}, \quad (19)$$

where $[Q]$ is given in ref. [12]. The corresponding stress-resultant matrix may be found from equation (2), i.e.,

$$\{\epsilon\} = [P] \{\epsilon\} = \sum_{n=0}^{\infty} [P] [B] \begin{Bmatrix} \delta_i \\ \delta_j \end{Bmatrix}, \quad (20)$$

where $[P]$ is the elasticity matrix for anisotropic shells.

The stiffness and mass matrices for one finite element are expressed as

$$[K] = \iint [B]^T [P] [B] dA, \quad [m] = \rho t \iint [N]^T [N] dA, \quad (21)$$

where $dA = r d\phi dx$, ρ is the density of the shell and t its thickness. Integrating over ϕ and using equations (18)-(20) we obtain

$$[k] = \left[[A]^{-1} \right]^T \left\{ \pi r \int_0^L [Q]^T [P] [Q] dx \right\} [A]^{-1} = \left[[A]^{-1} \right]^T [G] [A]^{-1} \quad (22)$$

$$[m] = \rho t \left[[A]^{-1} \right]^T \left\{ \pi r \int_0^L [R]^T [R] dx \right\} [A]^{-1} = \rho t \left[[A]^{-1} \right]^T [S] [A]^{-1} \quad (23)$$

where $[G]$ and $[S]$ are defined by the above equations.

$[G]$ and $[S]$ were obtained analytically for the case of isotropic shell in reference [12] by carrying out the necessary matrix operations and integrating over x in equations (22) and (23). To do this it was found necessary to introduce several intermediate matrices, eventually obtaining expressions for the general terms k_{ij} and m_{ij} of $[k]$ and $[m]$, respectively.

For the case of anisotropic shells, the elements of $[G]$ and $[S]$ are similar to those of reference [12], for the following reason: in [12], the (i,j) th terms of $[G]$ and $[S]$ are determined functions of the elements of $[P]$ and of the general terms, κ and μ , of the roots λ 's which have the same general form as those of equation (11). Because of the complexity of the manipulations, only the final result will be given here. The interested reader is referred to reference [12] for details.

The (i,j) th term of $[G]$ is given by

$$\begin{aligned}
\frac{2}{\pi r} \cdot G(i,j) = e^{A_1 \ell} & \left\{ \frac{[(D_1 - D_4)A_1 - (D_2 + D_3)(B_1 + C_1)] \cos [(B_1 + C_1)\ell]}{[A_1^2 + (B_1 + C_1)^2]} \right. \\
& + \frac{[(D_1 - D_4)(B_1 + C_1) + (D_2 + D_3)A_1] \sin [(B_1 + C_1)\ell]}{[A_1^2 + (B_1 + C_1)^2]} \\
& + \frac{[(D_1 + D_4)A_1 - (D_2 - D_3)(B_1 - C_1)] \cos [(B_1 - C_1)\ell]}{[A_1^2 + (B_1 - C_1)^2]} \\
& \left. + \frac{[(D_1 + D_4)(B_1 - C_1) + (D_2 - D_3)A_1] \sin [(B_1 - C_1)\ell]}{[A_1^2 + (B_1 - C_1)^2]} \right\} \\
& + \frac{(B_1 + C_1)(D_2 + D_3) - A_1(D_1 - D_4)}{[A_1^2 + (B_1 + C_1)^2]} \\
& + \frac{(B_1 - C_1)(D_2 - D_3) - A_1(D_1 + D_4)}{[A_1^2 + (B_1 - C_1)^2]}
\end{aligned} \tag{24}$$

for all $i, j = 1, 2, \dots, 8$, except for the following elements:

$$\begin{aligned}
& G(1,5), G(1,6), G(2,5), G(2,6), G(3,7), G(3,8), G(4,7), G(4,8), \\
& G(5,1), G(6,1), G(5,2), G(6,2), G(7,3), G(8,3), G(8,3), G(8,4)
\end{aligned}$$

which can be written as follows:

$$G(i,j) = \frac{\pi r}{2} \left[\frac{(D_1 - D_4) \sin(2B_1 \ell) + 2(D_2 + D_3) \sin^2(B_1 \ell)}{2B_1} + (D_1 + D_4)\ell \right] \tag{25}$$

In equations (24) and (25), $A_1, B_1, C_1, D_1, D_2, D_3, D_4$ represent the (i,j) th elements, correspondingly, of matrices $[A_1], [B_1], [C_1], [D_1], [D_2], [D_3]$ and $[D_4]$ which are given in reference [12].

Similarly, the (i,j) th term of $[S]$ is given by

$$\begin{aligned}
\frac{2}{\pi r} S(i,j) = e^{A_1 \ell} & \left\{ \frac{[(E_1 - E_4)A_1 - (E_2 + E_3)(B_1 + C_1)] \cos [(B_1 + C_1)\ell]}{[A_1^2 + (B_1 + C_1)^2]} \right. \\
& + \frac{[(E_1 - E_4)(B_1 + C_1) + (E_2 + E_3)A_1] \sin [(B_1 + C_1)\ell]}{[A_1^2 + (B_1 + C_1)^2]} \\
& + \frac{[(E_1 + E_4)A_1 - (E_2 - E_3)(B_1 - C_1)] \cos [(B_1 - C_1)\ell]}{[A_1^2 + (B_1 - C_1)^2]} \\
& \left. + \frac{[(E_1 + E_4)(B_1 - C_1) + (E_2 - E_3)A_1] \sin [(B_1 - C_1)\ell]}{[A_1^2 + (B_1 - C_1)^2]} \right\} \\
& + \frac{(B_1 + C_1)(E_2 + E_3) - A_1(E_1 - E_4)}{[A_1^2 + (B_1 + C_1)^2]} \\
& + \frac{(B_1 - C_1)(E_2 - E_3) - A_1(E_1 + E_4)}{[A_1^2 + (B_1 - C_1)^2]}
\end{aligned} \tag{26}$$

for all $i, j = 1, 2, \dots, 8$ except for the following elements

$$\begin{aligned}
& S(1,5), S(1,6), S(2,5), S(2,6), S(3,7), S(3,8), S(4,7), S(4,8) \\
& S(5,1), S(6,1), S(5,2), S(6,2), S(7,3), S(8,3), S(7,4), S(8,4)
\end{aligned}$$

which can be written as follows:

$$S(i,j) = \frac{\pi r}{2} \left[\frac{(E_1 - E_4) \sin(2B_1 \ell) + 2(E_2 + E_3) \sin^2(B_1 \ell)}{2B_1} + (E_1 + E_4)\ell \right] \tag{27}$$

Here again, E_1, E_2, E_3, E_4, B_1 and C_1 , in equations (26) and (27), represent the (i,j) th elements of the corresponding matrices given in reference [12].

2.5 Elasticity Matrix

The elasticity matrix $[P]$ given by equation (3) is quite general, so this theory may be applied to: (i) shells consisting of single or an arbitrary number of isotropic or orthotropic layers, (ii) double-walled, gridwork or folded shells and (iii) shells with rings and stringers provided their characteristics are known. Here we limit ourselves to shells consisting of single or an arbitrary number of isotropic or orthotropic layers symmetrically arranged relative to the coordinate surface.

For isotropic shells, the elements p_{ij} of $[P]$ are listed in reference [12]. In the case of an arbitrary number of orthotropic layers, we assume that these layers function concurrently without slippage and as previously stated that the principal directions of elasticity at each point of the shell coincide with the directions of coordinate lines; (i) for an even number of layers, $2v$, the elements p_{ij} of $[P]$ may be written in the form

$$p_{ij} = 2 \sum_{s=1}^v B_{ij}^s (t_s - t_{s+1}), \quad i=1 \text{ to } 3, \text{ and } j=1 \text{ to } 6,$$

$$p_{ij} = (2/3) \sum_{s=1}^v B_{i-3, j-3}^s (t_s^3 - t_{s+1}^3), \quad i=4 \text{ to } 6, \text{ and } j=4 \text{ to } 6. \quad (28)$$

(ii) for an odd number, $2v+1$, we obtain

$$p_{ij} = 2 \left[B_{ij}^{v+1} t_{v+1} + \sum_{s=1}^v B_{ij}^s (t_s - t_{s+1}) \right], \quad i=1 \text{ to } 3 \text{ and } j=1 \text{ to } 6$$

$$p_{ij} = (2/3) \left[B_{i-3, j-3}^{v+1} t_{v+1}^3 + \sum_{s=1}^v B_{i-3, j-3}^s (t_s^3 - t_{s+1}^3) \right], \quad i=4 \text{ to } 6 \text{ and } j=4 \text{ to } 6 \quad (29)$$

where

$$B_{11}^S = \left[E_1^S / (1 - \nu_1^S \nu_2^S) \right], B_{22}^S = \left[E_2^S / (1 - \nu_1^S \nu_2^S) \right],$$

$$B_{12}^S = B_{21}^S = \left[\nu_2^S E_1^S / (1 - \nu_1^S \nu_2^S) \right], B_{23}^S = 0.5G_{12}^S,$$

t_s is the coordinate of the s^{th} layer with respect to the middle surface as shown in Figure 2, (E_1^S, ν_1^S) and (E_2^S, ν_2^S) are its Young's modulus and Poisson's ratio in the x and ϕ directions, respectively, and G_{12}^S is the shear modulus. All other terms of B_{ij}^S are zero.

2.6 Stiffness and mass matrices for the whole shell in vacuo

As previously mentioned, the complete shell is divided into finite elements each of which is a cylindrical frustum (Fig. 3). The position of the nodal circles may be chosen arbitrary.

The vectors $\{F_i\}$, $\{F_j\}$ represent the internal forces acting at nodes i and j , respectively, and $\{\delta_i\}$ are the corresponding displacements. As the shell is continuous, the sum of forces and moments at a particular node must be equal to the external forces and moments applied at the node. Thus,

$$\{F\}^e = \{F_j\} + \{F_{i+1}\}$$

moreover, the displacement must be continuous, and

$$\{\delta_j\} = \{\delta_{i+1}\}.$$

These relationships allow us to superimpose the mass and stiffness matrices of individual finite elements, to obtain the global mass and stiffness matrices $[M]$ and $[K]$ for the whole shell in vacuo. This is shown diagrammatically in Fig. 3; $[K]$ and $[M]$ will be square matrices of order $4(N + 1)$, where N is the number of finite elements.

3. FREE VIBRATION

For free vibration, the equation of motion may be written in the form

$$[M] \{\ddot{\Delta}\} + [K] \{\Delta\} = \{0\}, \quad (30)$$

where $\{\Delta\} = \{\delta_1, \delta_2, \dots, \delta_{N+1}\}^T$, N is the number of finite elements, $[M]$ and $[K]$ are real, symmetric matrices of order $4(N+1) \times 4(N+1)$, and $\{\delta_{N+1}\}$ being the displacement vector associated with the lower edge of the last finite element.

In the cases where the shell has rigid edge constraints, the kinematic boundary conditions must be taken into consideration. Accordingly, $[K]$ and $[M]$ are reduced to square matrices of order $4(N+1)-J$, where J is the number of constraint equations imposed. Thus, for a shell with two edges supported, we must have $v_n = w_n = 0$ in the displacement vector $\{\delta_1\}$ and $\{\delta_{N+1}\}$ and $J = 4$; for a free shell, $J = 0$; and for one with two clamped edges $J = 8$. The solution of equation (30) now follows by standard matrix techniques, yielding the natural frequencies, ω_i , $i = 1, 2, \dots, 4(N+1)-J$ and the corresponding eigenvectors.

It must be stressed that the mass and stiffness matrices obtained are associated with a specific circumferential wave number, n , as is the nodal displacement vector. Thus the analysis is carried out independently for each n .

4. EFFECTS OF COMPRESSIBLE FLOW

When the fluid is flowing, the shell is subjected to inertia forces, centrifugal forces and coriolis-type forces coupled with the elastic deformation of its walls. The characteristics of the mathematical model to be used are as follows:

$$\left[[M] - [M_f] \right] \{\ddot{\Delta}\} - [C_f] \{\dot{\Delta}\} + \left[[K] - [K_f] \right] \{\Delta\} = \{0\}, \quad (31)$$

where $\{\Delta\}$ is a displacement vector, $[M]$ and $[K]$ are, respectively, the mass and stiffness matrices of the shell in vacuo, and $[M_f]$, $[C_f]$ and $[K_f]$, represent the inertia, coriolis and centrifugal forces of the flowing fluid. *on the shell*

$[M]$ and $[K]$ were obtained analytically by carrying out the necessary matrix operations eventually obtaining expressions (22) and (23) for the general terms of the mass and stiffness matrices for one finite element in vacuo, $[k]$ and $[m]$, respectively.

4.1 Mass, stiffness and damping matrices of the moving fluid

Consider now the way in which the shell interacts with the fluid. It is assumed that:

- (i) The flow is potential and the fluid compressible; furthermore, the limiting case of small vibrations will be considered.
- (ii) The pressure of the fluid on the walls is supposed to be purely lateral and the velocity distribution throughout the cross section

of the shell is also supposed to be constant.

- (iii) The internal pressures are not unduly high, so that pressurization of the shell is negligible. The general formulation of the problem will be carried out in the case of compressible fluid where both internal and external axial flows may be present, for the sake of generality.

The governing equation for the potential flow is given by

$$\nabla^2 \phi = (1/C^2) [\ddot{\phi} + 2U_x \dot{\phi}' + \phi''], = 0 \quad (32)$$

where C is the velocity of sound in fluid and U_x is the velocity of the fluid throughout the cross section of the shell; $(\dot{})$ and (\prime) stand for $\partial()/\partial t$ and $\partial()/\partial x$, respectively, and ϕ is the potential of the disturbances which is given by

$$V_x = U_x + \partial\phi/\partial x, \quad V_\phi = (1/r) (\partial\phi/\partial\phi), \quad V_r = \partial\phi/\partial r, \quad (33)$$

where V_x , V_ϕ and V_r are the components of the velocity field for disturbed motion.

The condition of impermeability of the surface of the shell and the dynamic condition of this surface which is given by Bernoulli's equation for disturbed motion, permit us to obtain the pressures of the fluid on the shell's walls as follows:

$$\begin{aligned} p_i &= -\rho_i (\dot{\phi}_i + U_{xi} \phi_i')_{r=a} , \\ p_e &= \rho_e (\dot{\phi}_e + U_{xe} \phi_e')_{r=a+t} , \end{aligned} \quad (34)$$

where a and t are the internal radius and the thickness of the shell element, respectively, the suffixes i and e indicate the internal and external region of the structure.

Finally the condition

$$(V_r)_{r=a} = \left(\frac{\partial \Phi}{\partial r}\right)_{r=a} = (\dot{W} + U_x \dot{W}')_{r=a} \quad (35)$$

must be satisfied at any point of the contact surface between the shell and the fluid.

Assuming that the displacement components have the form of equation (16) which satisfied the system of differential equation (5) and that

$$\Phi = \sum_{k=1}^8 R_k(r) S_k(x, \phi, \zeta), \quad (36)$$

we obtain the internal and external pressures as follows:

$$p = \sum_{k=1}^8 \left\{ \left[-\rho_i r_k + \rho_e s_k \right] \ddot{W}_k + 2a \left[-\rho_i U_{xi} r_k + \rho_e U_{xe} s_k \right] \dot{W}_k + a \left[-\rho_i U_{xi}^2 r_k + \rho_e U_{xe}^2 s_k \right] W_k \right\}, \quad (37)$$

acting on the shell's wall

where $W_k = C_k e^{i\lambda_k x/a + i\omega \zeta} \cos n\phi$, is given by equation (16), ρ is the density of the fluid, ω is the frequency and

$$\begin{aligned} r_k &= 1 / \left(n - im_k a \left(J_{n+1}(im_k a) / Y_n(im_k a) \right) \right), \\ s_k &= 1 / \left(n - im_k a \left(Y_{n+1}(im_k a) / Y_n(im_k a) \right) \right), \\ im_k a &= \left[-\lambda_k^2 + (a^2/c^2) \left(\frac{\lambda_k U_x}{a} + \omega \right)^2 \right]^{1/2}. \end{aligned} \quad (38)$$

and $J_n(im_k a)$ and $Y_n(im_k a)$ are, respectively, the Bessel functions of the first and second kind and of order n .

Introducing equation (18) into equation (37) by carrying out the necessary matrix operations of the finite element method and integrating over x and ϕ we obtain the inertia, centrifugal and coriolis of the moving fluid as follows:

$$\begin{bmatrix} m_f \\ 8 \times 8 \end{bmatrix} = \begin{bmatrix} A^{-1} \end{bmatrix}^T \begin{bmatrix} S_F \\ \end{bmatrix} \begin{bmatrix} A^{-1} \end{bmatrix}, \quad (39)$$

$$\begin{bmatrix} C_f \\ 8 \times 8 \end{bmatrix} = \begin{bmatrix} A^{-1} \end{bmatrix}^T \begin{bmatrix} D_F \\ \end{bmatrix} \begin{bmatrix} A^{-1} \end{bmatrix}, \quad (40)$$

and

$$\begin{bmatrix} k_f \\ 8 \times 8 \end{bmatrix} = \begin{bmatrix} A^{-1} \end{bmatrix}^T \begin{bmatrix} G_F \\ \end{bmatrix} \begin{bmatrix} A^{-1} \end{bmatrix}, \quad (41)$$

where

$$\begin{aligned} S_F(k,g) = & -\Pi \delta_i \gamma_i^2 r_g I_{kg}(1i,1j,a_i) \\ & + \Pi \delta_e \gamma_e^2 s_g I_{kg}(1i,1j,a_e), \end{aligned} \quad (42)$$

$$\begin{aligned} D_F(k,g) = & 2\lambda_g \Pi i \left[-\delta_i \bar{U}_i \gamma_i r_g I_{kg}(1i,1j,a_i) \right. \\ & \left. + \delta_e \bar{U}_e \gamma_e s_g I_{kg}(1i,1j,a_e) \right], \end{aligned} \quad (43)$$

$$\begin{aligned} G_F(k,g) = & (-\gamma_g^2 \Pi) \left[-\delta_i \bar{U}_i^2 r_g I_{kg}(1i,1j,a_i) \right. \\ & \left. + \delta_e \bar{U}_e^2 s_g I_{kg}(1i,1j,a_e) \right], \end{aligned} \quad (44)$$

and $k,g = 1, \dots, 8$.

In equations (42)-(44) the dimensionless quantities are defined as follows:

$$\begin{aligned}\delta_i &= (a_i/t_1)(\rho_i/\rho_1), & \delta_e &= (a_e/t_1)(\rho_e/\rho_1) \\ U_0^2 &= p(1,1,1)/\rho_1 t_1, & \bar{U}_e &= U_{xi}/U_0, & \bar{U}_e &= U_{xe}/U_0 \\ \gamma_i &= a_i/r_1, & \gamma_e &= a_e/r_1.\end{aligned}$$

where

ρ_1 , t_1 and r_1 are, respectively, the density, thickness and radius of the shell's element number one; $p(1,1,1)$ is the first terms of the elasticity matrix $[P]$; r_g and s_g are given by equation (38).

$$i^2 = -1; \quad I_{kg}(li, lj, a) = (lj - li)/a \quad \text{when} \quad \lambda_k + \lambda_g = 0 \quad \text{and}$$

$$I_{kg}(li, lj, a) = \frac{1}{i(\lambda_k + \lambda_g)} \left[e^{i(\lambda_k + \lambda_g) lj/a} - e^{i(\lambda_k + \lambda_g) li/a} \right]$$

otherwise.

With the mass, damping and stiffness matrices known for each fluid element, the global mass, damping and stiffness matrices for the whole column of fluid, $[M_f]$, $[C_f]$ and $[K_f]$, respectively, may be constructed by superposition in the normal manner. Between fluid elements continuity will be satisfied exactly by requiring an exact match of velocity normal to the element with the velocity of the adjacent element at all points on the interface. Each of these (square) matrices will be of order $4(N+1)$, where N is the total number of finite elements.

5. PRESSURE FLUCTUATIONS INDUCED BY INTERNAL FLOW

The dynamical behavior of the shell subjected to arbitrary loads may be governed by the following equation

$$\{[M] - [M_f]\} \{\ddot{y}\} + \{[C] - [C_f]\} \{\dot{y}\} + \{[K] - [K_f]\} \{y\} = \{F\}, \quad (45)$$

where $[C]$ is the damping matrix of the system; and $[M]$, $[M_f]$, $[K]$, $[K_f]$ and $[C_f]$ are given by equations (31).

The external forces $\{F\}$ represent the turbulent random pressure fluctuations at the shell's walls resulting from the passage of fully-developed turbulent flow. While this pressure field varies from point to point at any instant, its variation at any given point fluctuates irregularly with time, and the frequency spectrum results in many modes of vibration being excited with a statistical dependence between them. However, the forces of vibration can be represented by synthesis of the natural modes; this assumption is generally permissible only for such structures where nonlinearities can be ignored. ✓

The displacements are assumed small enough for the resultant forces to be normal to the shell's surface. It is also assumed that the pressure field is spatially continuous and that it has the properties of a weakly stationary, ergodic process. We further assumed that the pressure drop in the length of the shell is sufficiently small for the mean pressure to be considered constant over the length of the shell. Finally, the continuous random pressure field of the deformable body is approximated by a finite set of discrete forces and moments acting at the nodal points (Fig. 4). ?

This response due to random pressure field is developed by Lakis and Paidoussis (Ref. 13). Here we extend the theory by taking into account the effects of the inertia, centrifugal and coriolis forces of the moving fluid.

5.1 Representation of Pressure Field at Nodal Points

As previously mentioned, the shell is divided into N finite elements, each of which is a cylindrical frustum. The position of the $N+1$ nodal points may be chosen arbitrarily (Fig. 1).

Any pressure field is considered to be acting on an area s_e surrounding the node e of coordinate ℓ_e as shown in Figure 4 (a). We define the pressure distribution acting over this area s_e by two mutually perpendicular forces per unit length. We may write, for the actual resultant force per unit length,

$$F(x, \phi, t) = \sum_n f_{Rn}(x, t) \cdot \cos n\phi + \sum_n f_{Cn}(x, t) \cdot \sin n\phi, \quad (46)$$

where f_{Rn} and f_{Cn} are at a distance x_0 from the origin of the shell as shown in Figure 4 (a).

These two forces acting at point A are transformed to two forces and the moment, M_r , acting at the node e , as shown in Figure 4 (b).

The external force vector associated with the n^{th} circumferential wave number at a typical node e can now be written in the following form:

$$\{F(t)\}_e = \left\{ \begin{array}{l} 0 \\ l''_i \\ l'_i \\ l''_j \\ l'_j \\ l''_p \\ l'_p \end{array} \begin{array}{l} f_R(x_i, t) dx_i \\ (x_j - l_j) f_R(x_j, t) dx_j \\ f_C(x_p, t) dx_p \end{array} \right\}_e \quad (46)$$

where f_{Rn} and f_{Cn} are expressed in terms of the instantaneous pressure on the surface, $p(x, \phi, t)$.

5.2 Mean Square Response

We proceed by first considering the free vibration of the conservative system (30) and determining the natural frequencies ω_i and the eigenvectors $\{\phi_i\}$, $i = 1, 2, \dots, 4(N+1) - J$, where J is the number of kinematic boundaries.

We next form the modal matrix

$$[\Phi] = [\phi_1, \phi_2, \dots, \phi_{4(N+1)-J}], \text{ and define } \{y\} = [\Phi] \{Z\}. \quad (47), (48)$$

Finally the equations of motion (45) are decoupled and the mean square values of the displacements of the shell are expressed in terms of the axial and circumferential correlation functions of the pressure field, $\Psi_p(\xi, 0, 0)$ and $\Psi_p(0, \eta, 0)$ respectively; see equations (10)-(25) of reference [13].

In the case of subsonic boundary-layer pressure fluctuations, the streamwise and lateral spatial correlation functions have been examined theoretically and experimentally by Bakewell et al. [15] and Clinch [16].

Bakewell measured and derived expressions for the axial and circumferential correlation functions in experiments with air flowing in a cylindrical pipe. He found the following approximate expressions for the (real) spatial correlations:

$$\psi_{p\omega}(\xi, 0, 0) \approx e^{-b|S_\xi|} \cos a S_\xi, \quad (49)$$

$$\psi_{p\omega}(0, \eta, 0) \approx (1 + c S_\eta^2)^{-1} [2 - e^{-dS_\eta^2}]^{-1} \quad (50)$$

where $S_\xi = \xi\omega/U_{\text{conv}}$ and $S_\eta = \eta\omega/U_c$ are the axial and circumferential Strouhal number, $\xi = |x_i - x_j|$, $\eta = |r(\phi_i - \phi_j)|$, ω is the center frequency, and a, b, c, d are constants to be specified; U_{conv} and U_c are, respectively, the convection and the centerline velocities.

The values of the constants used in these two expressions for axial and circumferential correlations depend on the fluid. For turbulent flow in air, the values of a, b, c and d are given in [15].

$$\begin{aligned} a = 8.7266, \quad b = 1.0, \quad \text{for } S_\xi = \xi\omega/U_c \\ c = 20, \quad d = 100, \quad \text{for } S_\eta = \eta\omega/U_c \end{aligned} \quad (51)$$

Clinch measurements in water proved that these constants are approximately the same for different fluids at the same Strouhal number, at least for sufficiently high Reynolds number.

Upon using the experimentally based relations (49)-(51), we obtain the following expression for the mean square response of the shell [13]:

$$\begin{aligned} \overline{Y_q^2(t)} = & \sum_{r=1}^{4(N+1)-J} \phi_{qr}^2 \frac{r^2}{16\pi^2 \omega_r^4 M_r^2} \times \\ & \times \left[\sum_{i=1}^{N+1} \sum_{u=1}^{N+1} \phi_{ir} \phi_{ur} |\Gamma_{iu}^F| + 2 \sum_{i=1}^{N+1} \sum_{k=1}^{N+1} \phi_{ir} \phi_{kr} |\Gamma_{ki}^M| + \right. \\ & \left. + \sum_{j=1}^{N+1} \sum_{k=1}^{N+1} \phi_{jr} \phi_{kr} |\Gamma_{jk}^{MM}| + \sum_{p=1}^{N+1} \sum_{v=1}^{N+1} \phi_{pr} \phi_{vr} |\Gamma_{pv}^F| \right] \end{aligned} \quad (52)$$

where ϕ_{qr} is the $(qr)^{\text{th}}$ element of the modal matrix $[\Phi]$, M_r is the element of the generalized mass matrix, ω_r , the r^{th} natural frequency and r is the mean radius of the shell; Γ_{iu}^F , Γ_{ki}^M and Γ_{jk}^{MM} are derived analytically in reference [13].

Equation (52) is then the response of the shell to a subsonic boundary-layer pressure field at the nodal points $q(x, \phi)$. This response is associated with a specific n , where n is the circumferential wave number. By repeating the analysis for a sufficient number of n , the total response for any point on the nodal circles may be obtained by superposition, in accordance with the assumption that there is no coupling between the circumferential wave-numbers.

6. METHOD OF CALCULATION AND DISCUSSION

A computer program has been written in Fortran V Language for the CDC Cyber 74 computer, using single precision arithmetic throughout all the overlays. The input data for each finite element are the mean radius, r , wall thickness, t , length of the individual element, ℓ , material and fluid density, ρ and ρ_f , respectively, and the elements p_{ij} of $[P]$.

The necessary steps of the computational method may be outlined as follows for each element:

- a) We first specify the imposed boundary conditions, their number, J , and the values of n for which calculations should be done.
- b) The shell is then subdivided into a sufficient number, N , of finite elements.
- c) The eight complex roots, λ_p , of each characteristic equation (9) are calculated by Newton-Raphson iterative technique, and hence, we obtain $\kappa_1, \mu_1, \kappa_2, \mu_2, \alpha_j, \beta_j$ ($j=1, 2, \dots, 8$).
- d) The intermediate matrices $[R]$, $[A]$, and the mass and stiffness matrices, $[m]$ and $[k]$, of the shell in vacuo are determined.
- e) The mass, damping and stiffness matrices of the moving fluid $[m_f]$, $[c_f]$ and $[k_f]$, respectively, are computed by the relationships given by equations (39), (40) and (41).

When the mass, damping and stiffness matrices have thus been computed for each element, the global $[M]$, $[M_f]$, $[C]$, $[C_f]$, $[K]$ and $[K_f]$ are constructed and reduced appropriately to take account of the boundary conditions (Fig. 5).

For free vibration, the computer program proceeds to find the natural frequencies, ω_m , where $m=1, 2, \dots, 4(N+1) - J$ for each n , and the corresponding eigenvectors of a real square non-symmetric matrix of the special form $[M]^{-1} [K]$, where both $[M]$ and $[K]$ are real, symmetric matrices and $[M]$ is a positive definite.

Knowing the damping factor, the fluid velocity and its density at each mode of the structure, equation (31) permits us to obtain the effects of the inertia, coriolis and centrifugal forces on these eigenvalues; and relation (52) is finally executed to obtain the response to a boundary-layer pressure field.

6.1 Calculations

Some calculations were conducted to illustrate the theory. The first set of calculations was to test the effects of inertia, coriolis and centrifugal forces of the moving fluid on the natural frequencies of the vessel. The inertial effects of a stationary fluid contained by the shell were computed. This shell was first studied experimentally by Lindholm, Abramson and Kana (Ref. 17). It is a simply-supported shell constructed of 4130 steel tubing and filled with water. The pertinent data are as

follows: $r = 3.77$ cm, $t = 0.229$ mm, $L = 23.4$ cm, $\nu = 0.29$, $\rho_1/\rho = 0.128$. In the experiments, the liquid depth, b , was varied such that the fractional filling, b/L , took the value $b/L = 0, \frac{1}{4}, \frac{1}{2}, \frac{3}{4}$ and 1 . For each b/L , the natural frequencies and the W - component of the corresponding eigenvectors were measured, for a number of values of the circumferential wave-number, n , and of the number of axial half-waves, m .

The effects of inertial force were calculated by this theory assuming $U = 0$ in equations (42-44) and using 12 finite elements in the case of $b/L = 0, \frac{1}{4}, \frac{1}{2}, \frac{3}{4}$ and 1 . Figures 6 and 7 show some frequencies computed by Lindholm et al.; only those frequencies corresponding to combinations of n and m for which experimental data is available are shown here. Agreement between theory and experiment is quite good in most cases. *but $m=2$* → *OK Corrigé!*

We see that for $m = 1$ the frequency decrease rapidly with increasing b/L in the range $0 < b/L < 1/3$ approximately, and then decrease only slightly for higher fractional fillings. For higher m , however, the frequencies decrease appreciably with increasing b/L over the whole range of b/L , as might be expected.

The corresponding normalized eigenvectors for $n = 5$ and $m = 1$ and 2 are shown in figures 8 and 9. It is recalled that x is measured downwards in this theory, so that for partially filled shells the liquid-filled portion of the shell is on the right-hand side of the figures. We observe that small fractional filling produce the most pronounced distorting effect on the eigenvectors, as compared to the eigenvectors of the empty shell, par-

ticularly for $m = 1$ and 2 . This agrees with the corresponding effect on the natural frequencies. We note further that, for partially filled shells, the location of the nodes shifts towards the centre of mass of the system, i.e. towards the bottom; this is most noticeable for the case of $b/L = \frac{1}{2}$.

When the fluid is flowing, the shell will be subjected to centrifugal forces and coriolis-type forces. The former have the effect of diminishing the natural frequencies of the system, while the latter have a damping effect on vibrations in cases where one end of the shell is free. The magnitude of these effects depends on the dimensionless flow velocity \bar{U}_i . Unless we are dealing with rubber shells, very heavy fluids or very high velocities, the values of \bar{U}_i will be small and the effect of these forces will be correspondingly small. Thus for a steel cylindrical shell with $L/r = 26$ and $t/r = 0.023$ conveying air flow, $\bar{U}_i = 0.20$ corresponds to $U_x = 1000$ m/s. For this magnitude of flow velocity, the natural frequencies of the shell are found to diminish by only 3% as a result of the flow.

The second set of calculations undertaken was for a shell first studied by Clinch (Ref. 18). It is a thin, simply-supported cylindrical shell conveying water with flow velocities in the range (6.3-13.2 m/s), (248-520 in/s). The shell data are as follows: $r = 0.0762$ m, $L = 6.096$ m, $t = 6.35 \times 10^{-4}$ m, $E = 1.965 \times 10^{11}$ Nm⁻², $\nu = 0.305$, $\rho = 8.0048 \times 10^3$ kg.m⁻³. Clinch obtained experimental data of the mean square radial displacement of the shell in the frequency range of 100-1,000 Hz, approximately. Moreover, the experimental values of the mean square radial displacements given by Clinch are mean values of measurements taken at several locations on the shell.

with very thin shells?

Why (and how) ignore below 150 Hz?

This shell was analysed by this theory by subdividing the shell into 8 identical finite elements. The natural frequencies of the shell for $n = 2$ and $n = 3$ were below 100 Hz, indicating that the high frequency response as measured by Clinch would likely differ appreciably from the total response.

Calculations of the response were confined to $n = 2$ to 12 from which the total response of this theory are shown in Figure 10 in terms of the radial, axial and circumferential displacements. The results indicate that the total R.M.S. radial displacement response is proportional to flow velocity raised to the 2.7 power.

The values of this total R.M.S. radial displacement response of the shell at its axial mid-point are also shown in Figure 11. Also shown in Figure 11 are values of the high-frequency response, as calculated by this theory, obtained by taking into account only the modes whose natural frequencies are in the range 93-1,000 Hz; also shown are Clinch's experimental results.

It is evident from Figure 11 that the response at the high frequency range is but a small part of the total. Thus, at the flow velocity of 6.3 m/s (248 in/s) the total mean square response is $2.0645 \times 10^{-11} \text{ m}^2$ ($3.2 \times 10^{-8} \text{ in}^2$) whereas the high-frequency response is $5.161 \times 10^{-14} \text{ m}^2$ ($8 \times 10^{-11} \text{ in}^2$), approximately, giving a ratio of 20/1 for the corresponding R.M.S. values; the difference at higher flow velocities is even more pronounced. The second point of interest in figure 8 is that agreement between this theory and experiment, in the frequency range of 100-1,000 Hz approximately, is quite good.

7. CONCLUSION

The theory developed in this paper is used to obtain the effects of inertia, coriolis and centrifugal forces of the moving fluid on the vibration characteristics of anisotropic cylindrical shells; and to predict the response to an arbitrary random pressure field. To this end the shell is subdivided into a number of cylindrical finite elements, each with two nodes, the nodal displacements being the axial circumferential and radial displacements and a rotation. The pressure field is similarly rendered discrete and is represented by two forces and a moment at each node.

This theory was computerized so that if the dimensions and material properties of each element, and the properties and the flow velocity of the fluid, are given as inputs, the program gives as output the natural frequencies and eigenvectors of the shell; the effects of inertia, coriolis and centrifugal forces of the moving fluid and the R.M.S. values of the nodal displacements.

The necessary time for the calculation of R.M.S. response for a typical case involving six finite elements is approximately ten minutes. This CPU time seems to be high. The time quoted above refers to the case where all the computed natural frequencies are used in the calculation of response. However if only a few of the lowest natural frequencies are used in the calculation, the response may be computed to an acceptable degree of accuracy, but with considerable saving in computational cost; thus, if only 20% of the natural frequencies are utilized, then the time given above may be re-

duced by a factor of $1/11$, approximately. Moreover the computer calculation involves the determination of $(\bar{u}_n^2)^{\frac{1}{2}}$, $(\bar{w}_n^2)^{\frac{1}{2}}$, $(\overline{dw_n/dx})^2$ and $(\bar{v}_n^2)^{\frac{1}{2}}$ at every nodal point. Accordingly, large savings in time may be realized if the response is not required at every node, or if only the RMS radial displacement is desired. Also, the computational difficulties in classical analysis arising from the vanishing determinant of the boundary conditions, which contains both large and small terms of the type $e^{\pm\lambda_i l/r}$, are not encountered here; difficulties due to such terms in this theory are easily overcome either by increasing N or by matrix manipulations.

This theory does not take into account pressurization of the shell; however, the theory can be extended to take this into account fairly easily. The main advantage of this theory is that it may be used, without modification, to obtain the effects of fluid pressures on the vibration characteristics of anisotropic cylindrical shells, no matter how many property discontinuities may be present, and for whatever boundary conditions. In this connection, it should be noted that this theory is equally applicable to cases where the shell is subjected to an external, as well as internal, pressure field, including the case where the pressure field arises from an external axial flow.

ACKNOWLEDGEMENTS

This research is supported by the National Research Council of Canada (Grant No. A8814) whose assistance is hereby gratefully acknowledged. The author wishes to express his thanks to Mlle Nicole Dontigny for typing this paper.

APPENDIX I

Matrix [R]

$$\begin{bmatrix}
 e^{-\psi_1}[\bar{\alpha}_1 \cos \zeta_1 - \bar{\alpha}_2 \sin \zeta_1] & e^{-\psi_1}[\bar{\alpha}_2 \cos \zeta_1 + \bar{\alpha}_1 \sin \zeta_1] & e^{-\psi_2}[\bar{\alpha}_3 \cos \zeta_2 - \bar{\alpha}_4 \sin \zeta_2] & e^{-\psi_2}[\bar{\alpha}_4 \cos \zeta_2 + \bar{\alpha}_3 \sin \zeta_2] \\
 e^{-\psi_1}[\bar{\beta}_1 \cos \zeta_1 - \bar{\beta}_2 \sin \zeta_1] & e^{-\psi_1}[\bar{\beta}_2 \cos \zeta_1 + \bar{\beta}_1 \sin \zeta_1] & e^{-\psi_2}[\bar{\beta}_3 \cos \zeta_2 - \bar{\beta}_4 \sin \zeta_2] & e^{-\psi_2}[\bar{\beta}_4 \cos \zeta_2 + \bar{\beta}_3 \sin \zeta_2] \\
 e^{\psi_1}[\bar{\alpha}_5 \cos \zeta_1 - \bar{\alpha}_6 \sin \zeta_1] & e^{\psi_1}[\bar{\alpha}_6 \cos \zeta_1 + \bar{\alpha}_5 \sin \zeta_1] & e^{\psi_2}[\bar{\alpha}_7 \cos \zeta_2 - \bar{\alpha}_8 \sin \zeta_2] & e^{\psi_2}[\bar{\alpha}_8 \cos \zeta_2 + \bar{\alpha}_7 \sin \zeta_2] \\
 e^{\psi_1}[\bar{\beta}_5 \cos \zeta_1 - \bar{\beta}_6 \sin \zeta_1] & e^{\psi_1}[\bar{\beta}_6 \cos \zeta_1 + \bar{\beta}_5 \sin \zeta_1] & e^{\psi_2}[\bar{\beta}_7 \cos \zeta_2 - \bar{\beta}_8 \sin \zeta_2] & e^{\psi_2}[\bar{\beta}_8 \cos \zeta_2 + \bar{\beta}_7 \sin \zeta_2]
 \end{bmatrix}$$

$$\omega_j = \kappa_j l/r, \quad \eta_j = \mu_j l/r, \quad \psi_j = \kappa_j x/r, \quad \zeta_j = \mu_j x/r; \quad j = 1, 2,$$

Matrix [A]

$$\begin{bmatrix}
 \bar{\alpha}_1 & \bar{\alpha}_2 & \bar{\alpha}_3 & \bar{\alpha}_4 & \bar{\alpha}_5 & \bar{\alpha}_6 & \bar{\alpha}_7 & \bar{\alpha}_8 \\
 1 & 0 & 1 & 0 & 1 & 0 & 1 & 0 \\
 -\kappa_1/r & \mu_1/r & -\kappa_2/r & \mu_2/r & \kappa_1/r & \mu_1/r & \kappa_2/r & \mu_2/r \\
 \bar{\beta}_1 & \bar{\beta}_2 & \bar{\beta}_3 & \bar{\beta}_4 & \bar{\beta}_5 & \bar{\beta}_6 & \bar{\beta}_7 & \bar{\beta}_8 \\
 e^{-\omega_1}[\bar{\alpha}_1 \cos \eta_1 - \bar{\alpha}_2 \sin \eta_1] & e^{-\omega_1}[\bar{\alpha}_2 \cos \eta_1 + \bar{\alpha}_1 \sin \eta_1] & e^{-\omega_2}[\bar{\alpha}_3 \cos \eta_2 - \bar{\alpha}_4 \sin \eta_2] & e^{-\omega_2}[\bar{\alpha}_4 \cos \eta_2 + \bar{\alpha}_3 \sin \eta_2] & e^{\omega_1}[\bar{\alpha}_5 \cos \eta_1 - \bar{\alpha}_6 \sin \eta_1] & e^{\omega_1}[\bar{\alpha}_6 \cos \eta_1 + \bar{\alpha}_5 \sin \eta_1] & e^{\omega_2}[\bar{\alpha}_7 \cos \eta_2 - \bar{\alpha}_8 \sin \eta_2] & e^{\omega_2}[\bar{\alpha}_8 \cos \eta_2 + \bar{\alpha}_7 \sin \eta_2] \\
 e^{-\omega_1} \cos \eta_1 & e^{-\omega_1} \sin \eta_1 & e^{-\omega_2} \cos \eta_2 & e^{-\omega_2} \sin \eta_2 & e^{\omega_1} \cos \eta_1 & e^{\omega_1} \sin \eta_1 & e^{\omega_2} \cos \eta_2 & e^{\omega_2} \sin \eta_2 \\
 \frac{e^{-\omega_1}}{r}[-\kappa_1 \cos \eta_1 - \mu_1 \sin \eta_1] & \frac{e^{-\omega_1}}{r}[\mu_1 \cos \eta_1 - \kappa_1 \sin \eta_1] & \frac{e^{-\omega_2}}{r}[-\kappa_2 \cos \eta_2 - \mu_2 \sin \eta_2] & \frac{e^{-\omega_2}}{r}[\mu_2 \cos \eta_2 - \kappa_2 \sin \eta_2] & \frac{e^{\omega_1}}{r}[\kappa_1 \cos \eta_1 - \mu_1 \sin \eta_1] & \frac{e^{\omega_1}}{r}[\mu_1 \cos \eta_1 + \kappa_1 \sin \eta_1] & \frac{e^{\omega_2}}{r}[\kappa_2 \cos \eta_2 - \mu_2 \sin \eta_2] & \frac{e^{\omega_2}}{r}[\mu_2 \cos \eta_2 + \kappa_2 \sin \eta_2] \\
 e^{-\omega_1}[\bar{\beta}_1 \cos \eta_1 - \bar{\beta}_2 \sin \eta_1] & e^{-\omega_1}[\bar{\beta}_2 \cos \eta_1 + \bar{\beta}_1 \sin \eta_1] & e^{-\omega_2}[\bar{\beta}_3 \cos \eta_2 - \bar{\beta}_4 \sin \eta_2] & e^{-\omega_2}[\bar{\beta}_4 \cos \eta_2 + \bar{\beta}_3 \sin \eta_2] & e^{\omega_1}[\bar{\beta}_5 \cos \eta_1 - \bar{\beta}_6 \sin \eta_1] & e^{\omega_1}[\bar{\beta}_6 \cos \eta_1 + \bar{\beta}_5 \sin \eta_1] & e^{\omega_2}[\bar{\beta}_7 \cos \eta_2 - \bar{\beta}_8 \sin \eta_2] & e^{\omega_2}[\bar{\beta}_8 \cos \eta_2 + \bar{\beta}_7 \sin \eta_2]
 \end{bmatrix}$$

APPENDIX II

R E F E R E N C E S

1. Naumann, E.C. "On the prediction of vibration behavior of free-free truncated conical shells", NASA tech. Note D-4772, 1968.
2. Sewall, J.L. and Naumann, E.C. "An experimental and analytical vibration study of thin cylindrical shells with and without longitudinal stiffeners", NASA tech. note D-4705.
3. Cohen, G.A. "Computer analysis of asymmetric free vibrations of ring-stiffened orthotropic shells of revolution", Am. Inst. Aeronaut. Astronaut. J1.1965, 3, 2305.
4. Cooper, P.A. "Vibration and buckling of prestressed shells of revolution", NASA tech. note D-3831, 1967.
5. Popov, E.P., Penzien, J. and Lu, Z.A. "Finite element solution for axisymmetric shells", Proc. Am. Soc. Civ. Engrs EM 5, 1964, 90, 119.
6. Jones, R.E. and Strome, D.R. "Direct stiffness method of analysis of shells of revolution utilizing curved elements", Am. Inst. Aeronaut. Astronaut. J1.1966, 4, 1519.
7. Percy, J.H., Plan, T.H., Klein, S. and Navaratna, D.R. "Application of matrix displacement method to linear elastic analysis of shells of revolution", Am. Inst. Aeronaut. Astronaut. J1.1965, 3, 2138.

8. Jones, R.E. and Strome, D.R. "A survey of analysis of shells by the displacement method", Proc. Conf. Matrix Meth. Struct. Mech. 1965 (Wright-Patterson Air Force Base, Ohio).
9. Webster, J.J. "Free vibrations of shells of revolution using ring finite elements", Int. J. mech. Sci. 1967, 9, 559.
10. Bacon, M.D. and BERT, C.W. "Unsymmetrical free vibrations of orthotropic sandwich shells of revolution", Am. Inst. Aeronaut. Astronaut. Jl. 1967, 5, 413.
11. Forsberg, K. "Influence of boundary conditions on the modal characteristics of thin cylindrical shells", Am. Inst. Aeronaut. Astronaut. Jl. 1964, 2, 2150.
- J 12. Lakis, A.A. and Paidoussis, M.P. "Dynamic analysis of axially non-uniform thin cylindrical shells". Journal of Mechanical Engineering Science, 14, pp. 49-71 (1972).
- J 13. Lakis, A.A. and Paidoussis, M.P. "Prediction of the response of a cylindrical shell to arbitrary or boundary-layer-induced random pressure fields". Journal of Sound and Vibration, 25, pp. 1-27 (1972).
14. Sanders, J.L. "An improved first approximation theory for thin shells", NASA tech. Rep. R24, 1959.
15. Bakewell Jr., H.P. Carey, G.F., Libuha, J.J., Schloemer, H.H. and Von Winkle, W.A. "Wall pressure fluctuations in turbulent pipe flow". U.S. Navy Underwater Sound Lab. Report No. 559 (1962).

16. Clinch, H.M. "Measurements of the wall pressure field at the surface of a smooth-walled pipe containing turbulent water-flow". *Journal of Sound and Vibration*, 9, pp. 398-420 (1962).
17. Lindholm, U.S., Kana, D.D. and Abramson, H.V. "Breathing vibrations of a circular cylindrical shell with an internal liquid". *Journal of Aeronautical Science*, 29, pp. 1052-1059 (1962).
18. Clinch J.M. "Prediction and measurement of the vibrations induced in thin-walled pipes by the passage of internal turbulent water flow". *Journal of Sound and Vibration*, 12, pp. 429-451 (1970).

APPENDIX III

NOTATION

a	internal radius of the shell
a,b,c,d	constants defined by equation (51)
b/L	liquid depth ratio
c	velocity of sound in fluid
E	Young's modulus
e	exponential
i	$i^2 = -1$
J_n	Bessel function of the first kind and of order n
ℓ	length of finite element
L	total length of shell
m	axial half-wave number
n	circumferential wave number
$N_x, N_\phi, N_{x\phi}$	
$M_x, M_\phi, M_{x\phi}$	stress resultants for a circular cylinder
p_i, p_e	internal and external pressure
p_{ij}	elements of elasticity matrix $[P]$
r	mean radius of shell
r_1	mean radius of shell's element number one
r_k, s_k	expressions given by equation (38)
s_ξ, s_η	axial and circumferential strouhal number
t	wall-thickness of shell
t_1	wall-thickness of shell's element number one
U,V,W	axial tangential and radial displacements

U_c	centerline velocity
$U_o, \bar{U}_i, \bar{U}_e$	expressions given by equations (42)-(44)
x	axial coordinate
Y_n	Bessel function of the second kind and of order n
$[A]$	defined by equation (17)
$[B]$	defined by equation (19)
$[A_j], [B_j], [C_j], [D_j]$, $j=1, \dots, 4$	defined by equation (24)
$[E_j]$, $j=1, \dots, 4$	defined by equation (26)
$[C_f], [C]$	damping matrices defined by equation (45)
$\{F\}$	represent the internal random pressure field
$[G]$	defined by equation (26)
$[k]$	stiffness matrix for one finite element
$[k_f]$	stiffness matrix for one fluid finite element
$[K]$	stiffness matrix for the whole shell
$[K_f]$	stiffness matrix for the whole fluid column
$[m], [m_f]$	mass matrices for the shell and fluid finite element, respectively
$[M]$	mass matrix of the whole shell in vacuo
$[N]$	defined by equation (18)
$[P]$	elasticity matrix
$[Q]$	defined by equation (19)
$[R]$	defined by equation (16)
$[S]$	defined by equation (26)

- $[T]$ defined by equation (6)
 $\{y\}, \{z\}$ displacement vectors defined by equation (1)
 $\{\delta_i\}, \{\delta_j\}$ nodal displacement vector defined by equation (6)
 $[\phi]$ modal matrix
 $\{\epsilon\}$ strain vector
 $\alpha_j, \beta_j, \bar{\alpha}_j, \bar{\beta}_j, j=1, \dots, 8$ defined by equation (15)
 $\kappa_j, \mu_j \quad j=1, 2$ real and imaginary parts of λ_p
 $\kappa_x, \kappa_\phi, \bar{\kappa}_{x\phi}$ axial, circumferential and twisting strains
 $\gamma_i, \gamma_e, \gamma_i = a_i/r_1, \quad \gamma_e = a_e/r_1$
 δ_i, δ_e defined by equation (44)
 η equal to $|r(\phi - \phi^1)|$
 λ roots of characteristic equation
 ν Poisson's ratio
 ξ equal to $|x - x^1|$
 ρ density of material of the shell
 ρ_i, ρ_e density of internal and external fluid
 ϕ circumferential coordinate
 Φ potential of the disturbances
 $\Psi_p(\xi, 0, 0), \psi(0, \eta, 0)$ longitudinal and lateral correlation functions of the fluctuating pressure
 ω_r r th natural frequency

APPENDIX IV

FIGURES

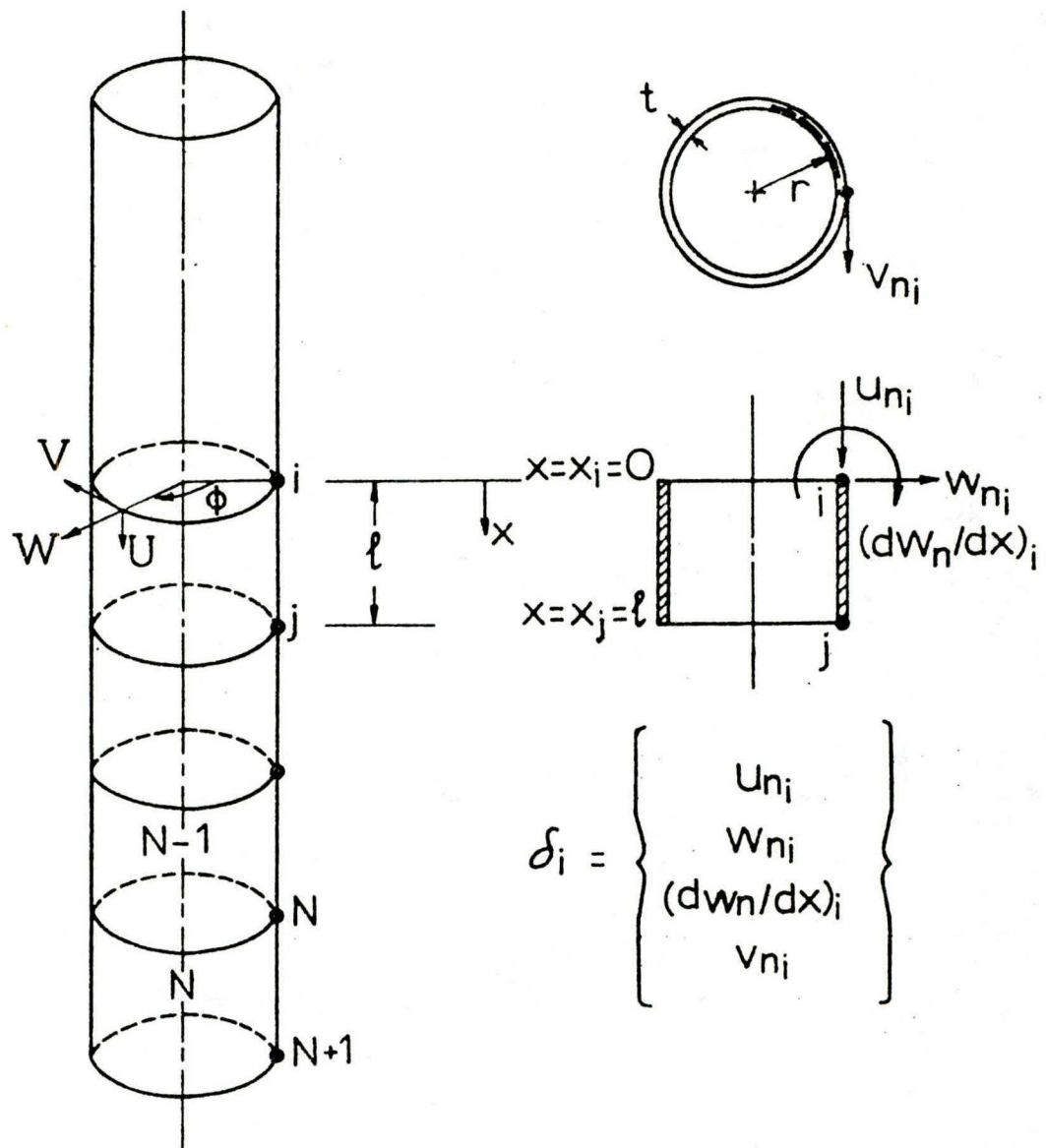


FIGURE 1 Definitions of the finite element used and of the displacement vector δ_i .

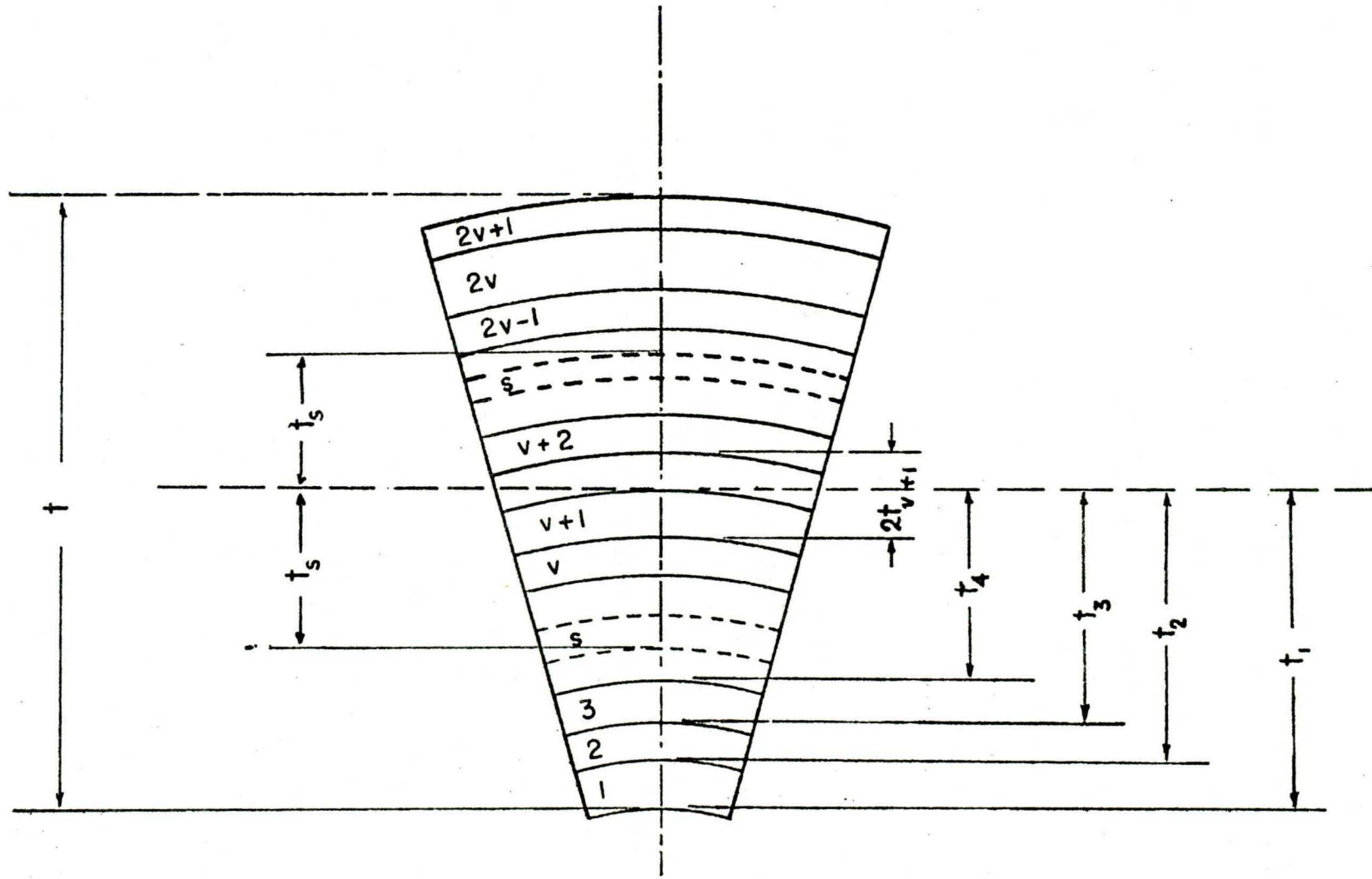


FIGURE 2 Shells consisting of odd number ($2v+1$) of anisotropic layers.

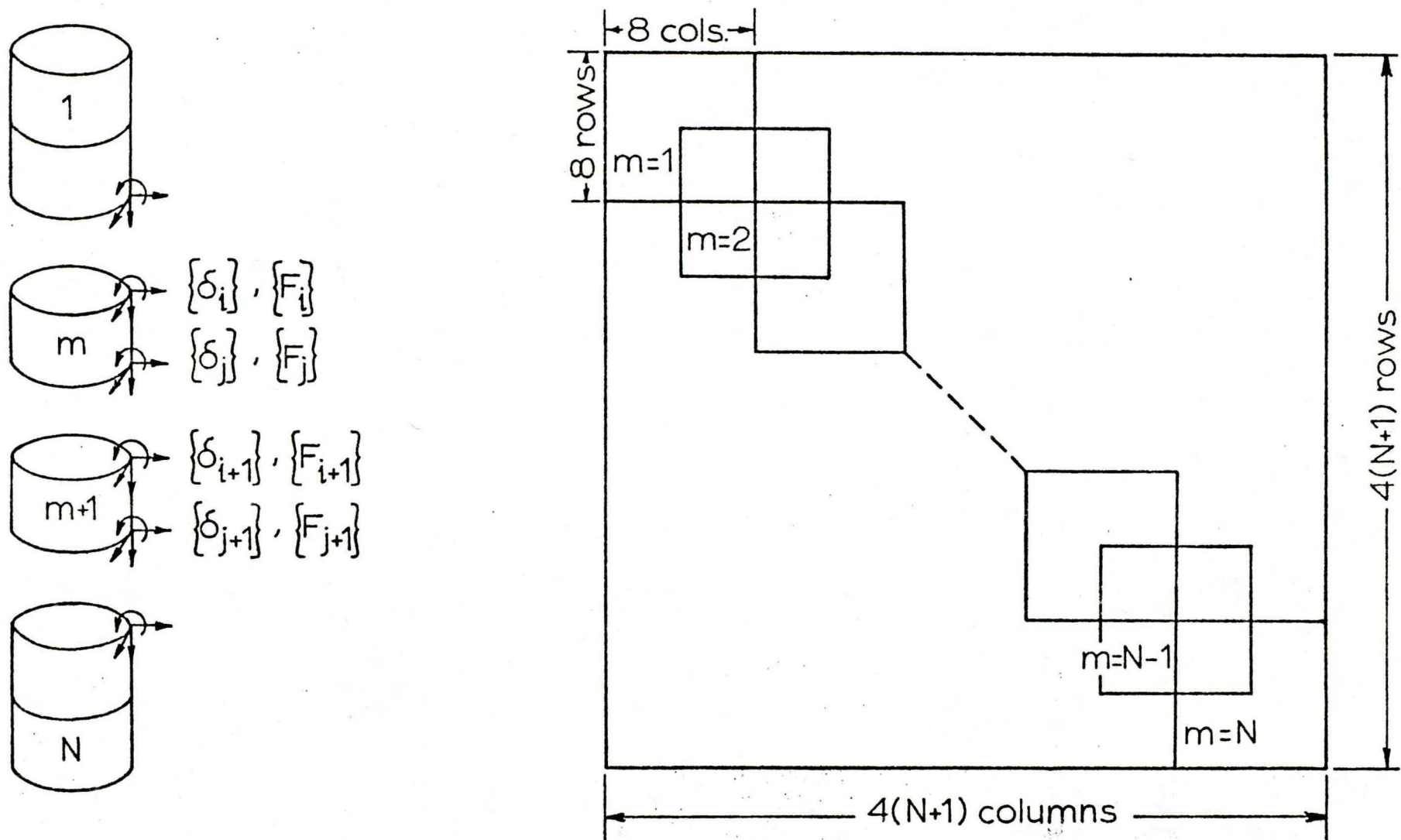


FIGURE 3.

Illustration of the construction of stiffness and mass matrices for the whole shell. (N = number of elements).

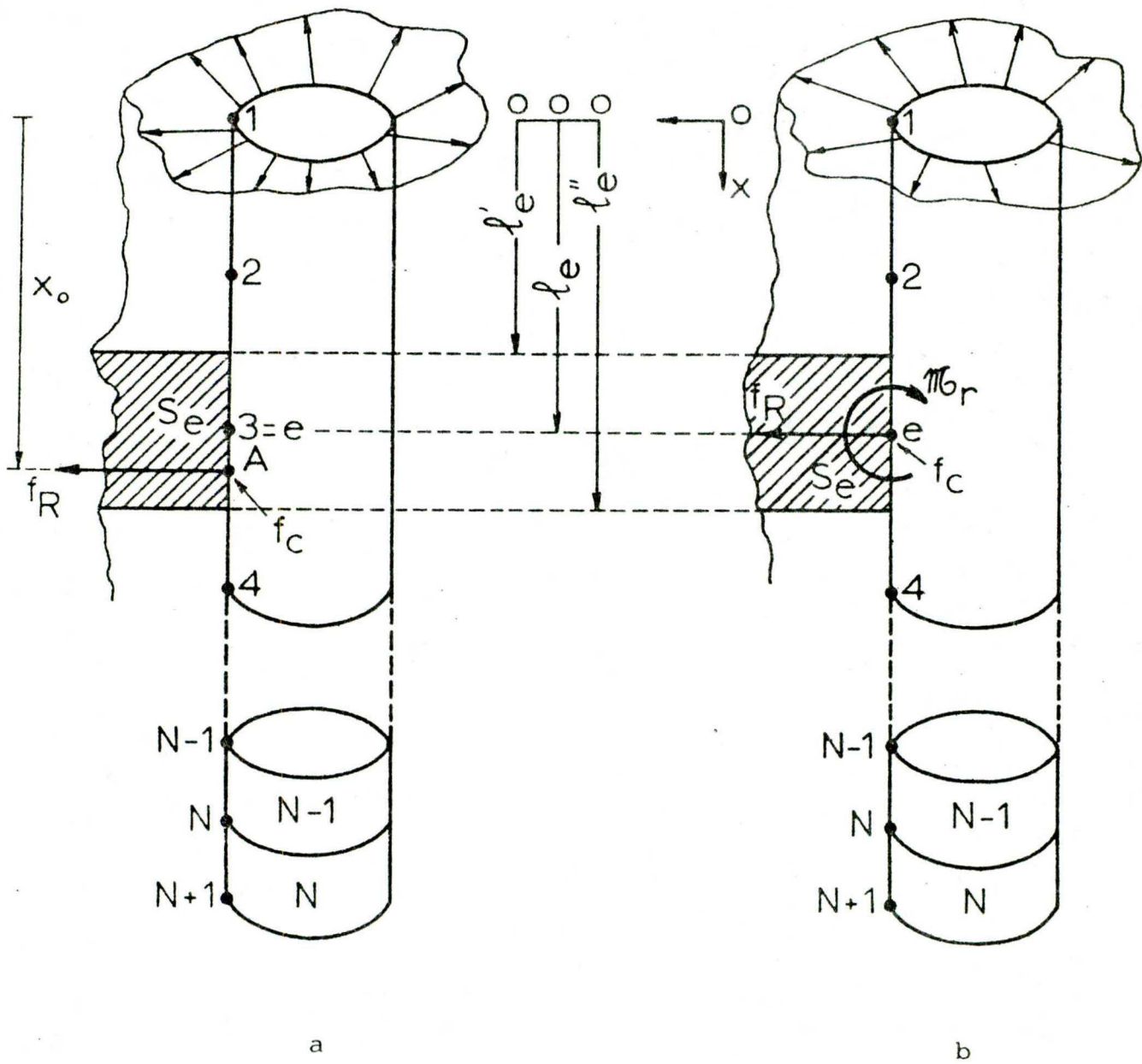


FIGURE 4 (a) Transformation of the continuous pressure field to a discrete force field

(b) The equivalent discrete force field acting at the node, e , involving f_R , f_C and M_r .

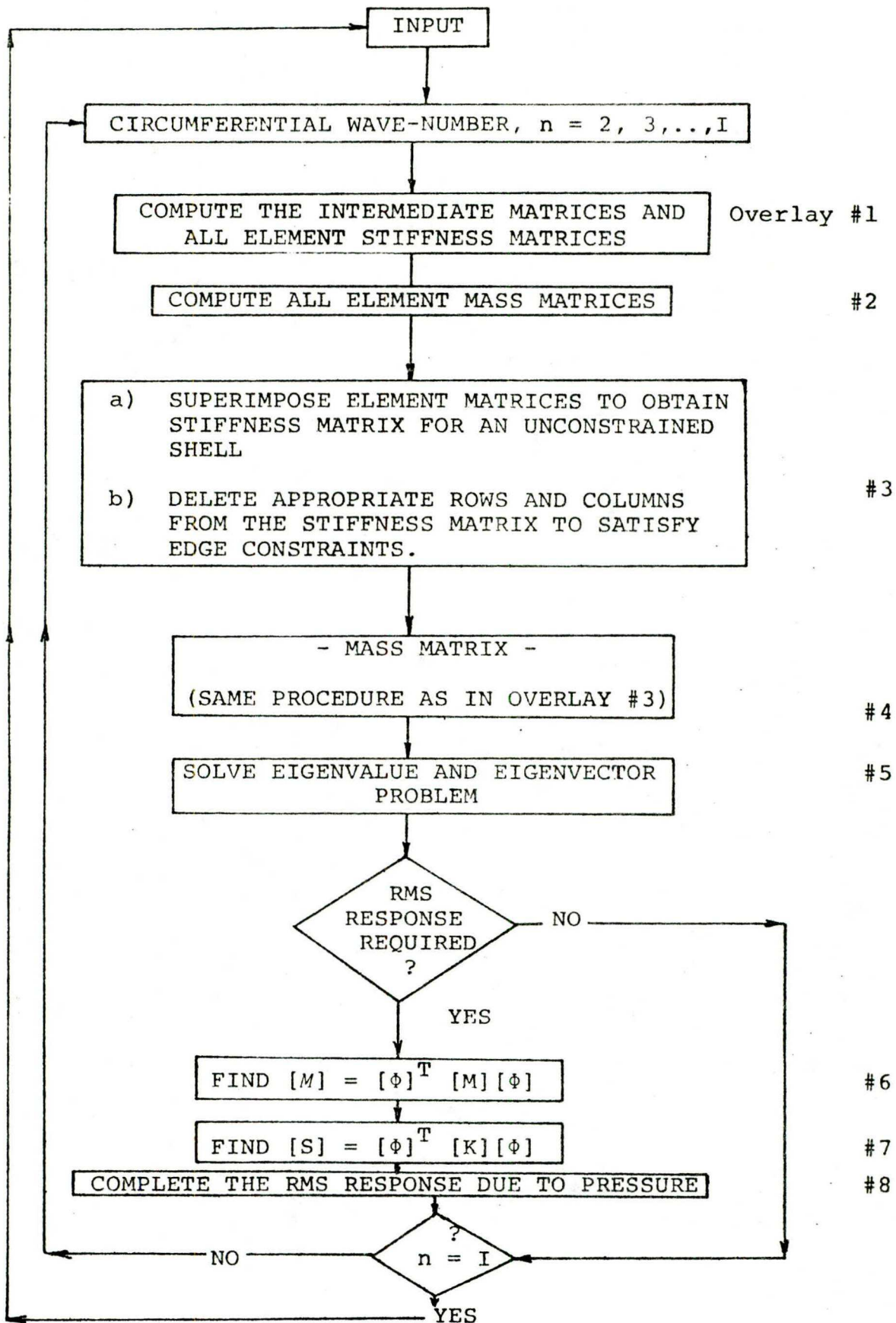


FIGURE 5. Computational flow diagram.

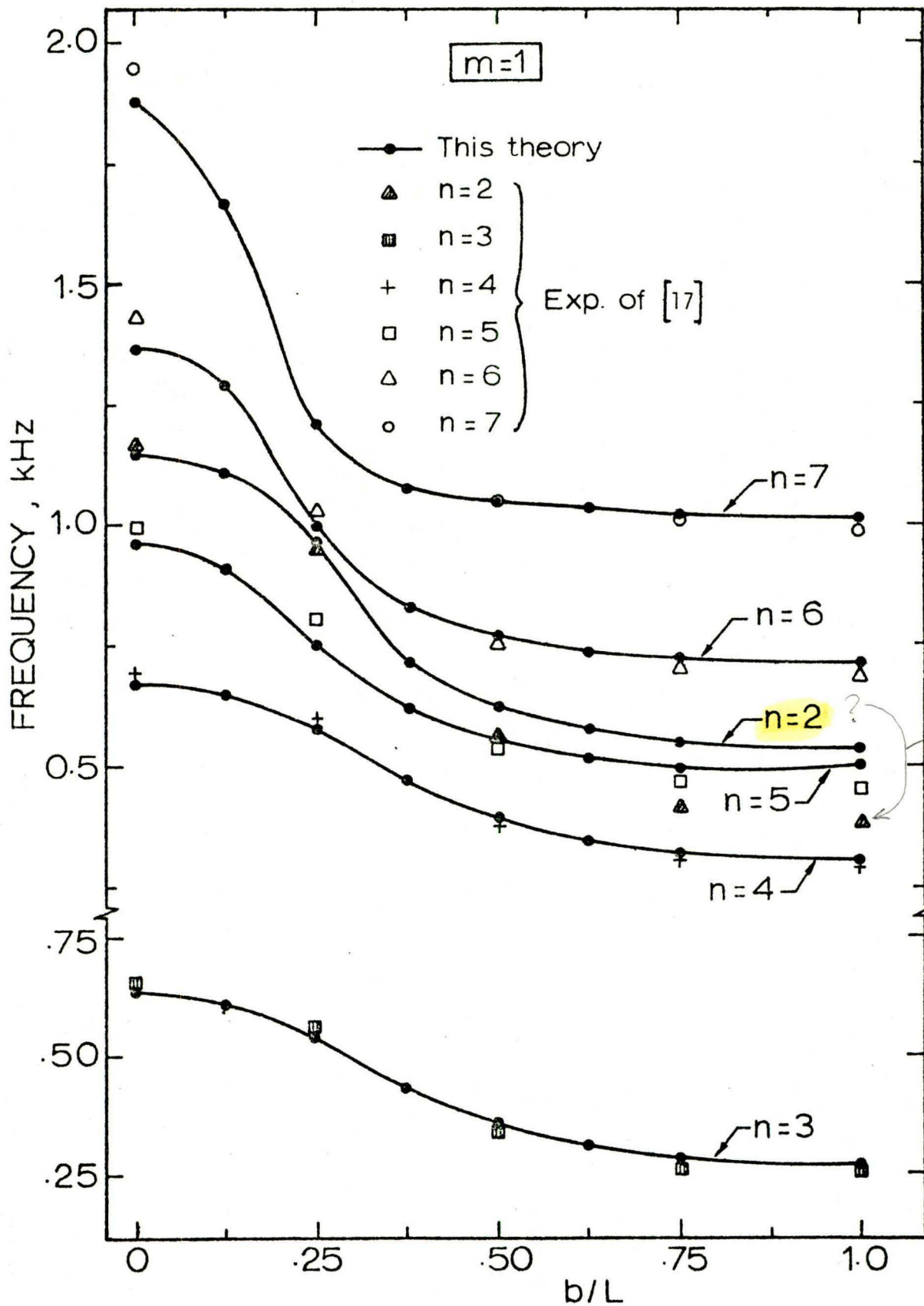


FIGURE 6

Comparison of this theory with experiments of for liquid-filled shells; $m = 1$.

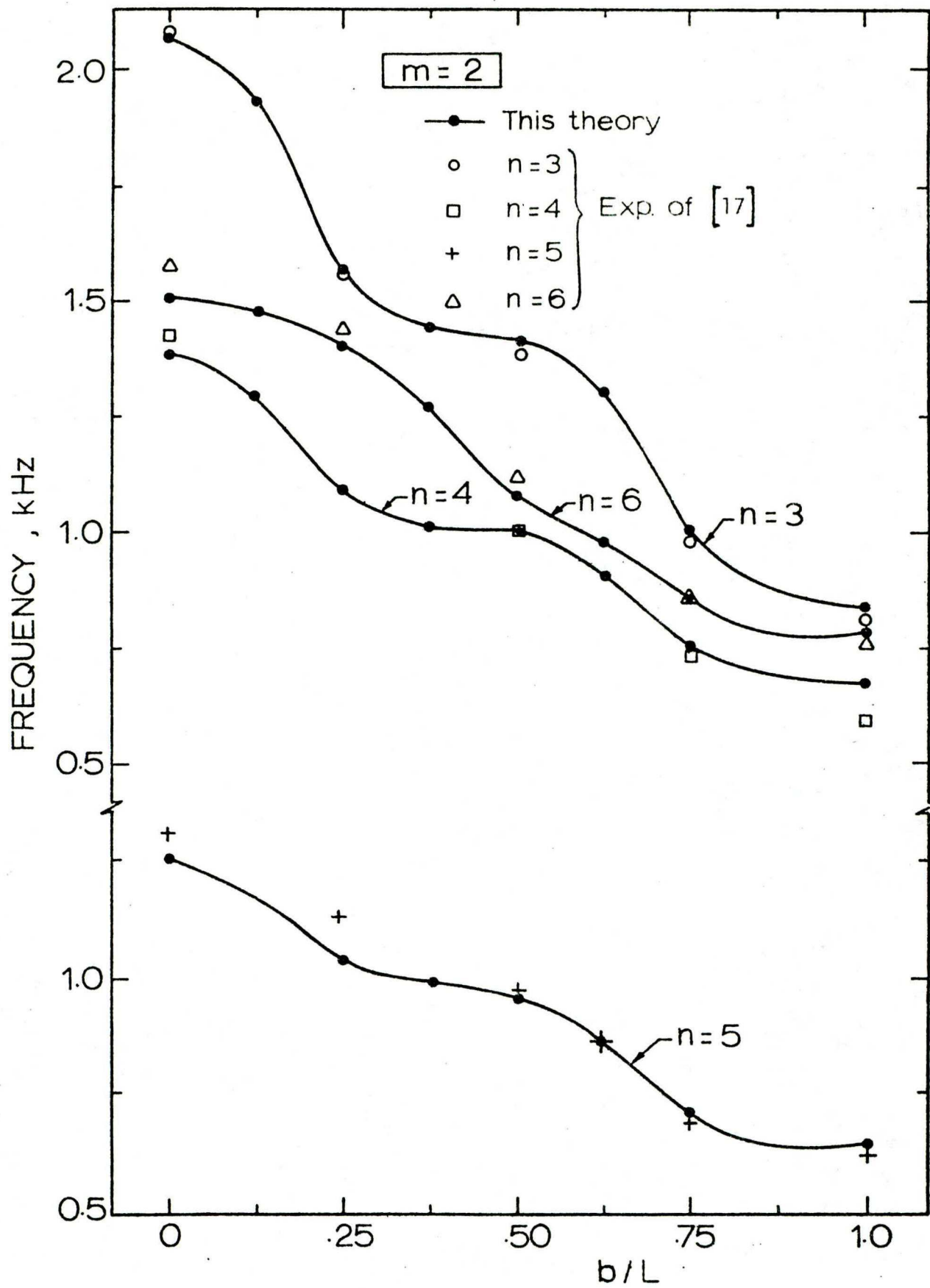


FIGURE 7

Comparison of this theory with experiments of for liquid-filled shells; $m = 2$.

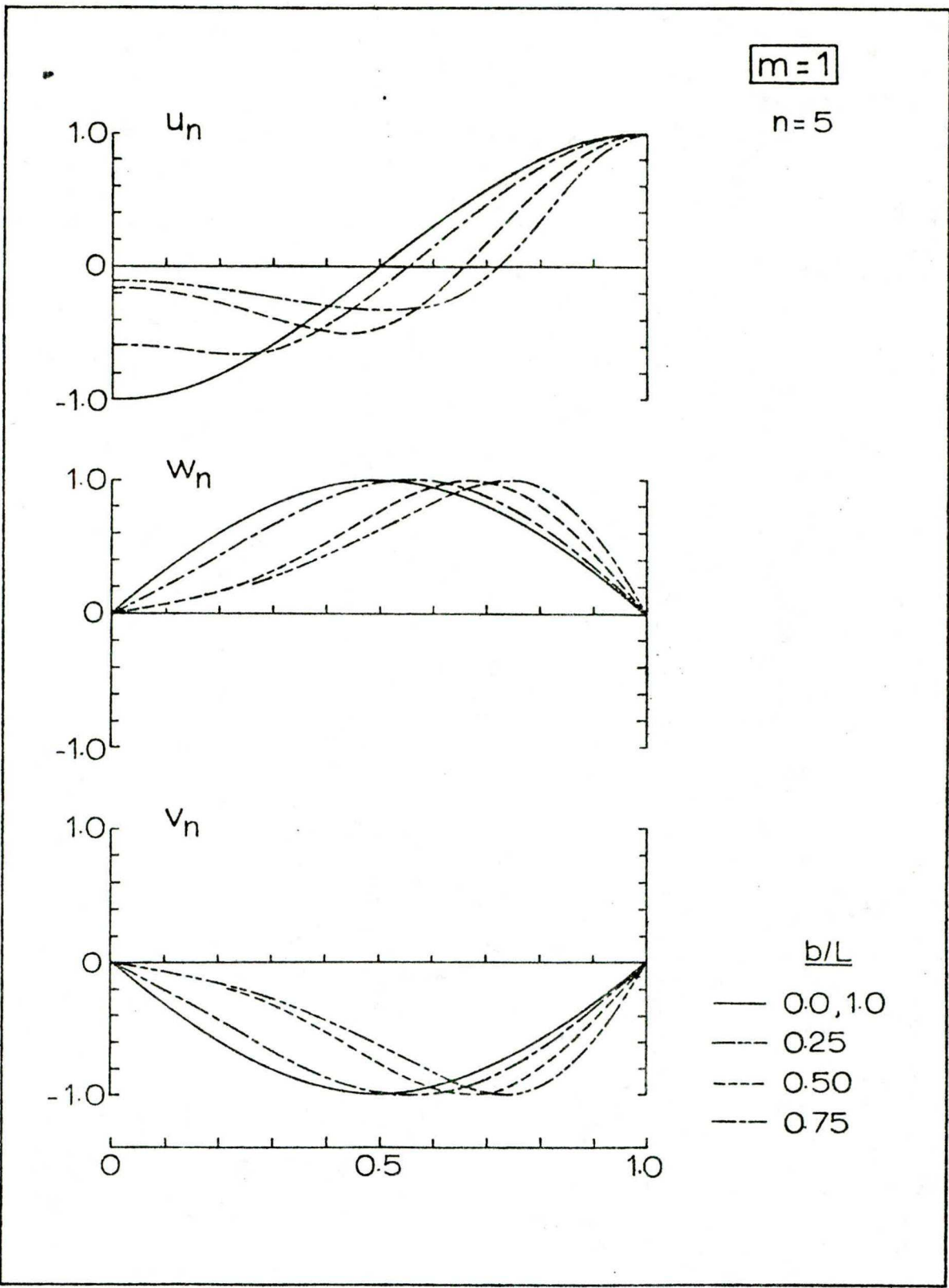


FIGURE 8 Eigenvectors of liquid-filled shells, as functions of liquid depth, b ; for $n = 5$, $m = 1$.

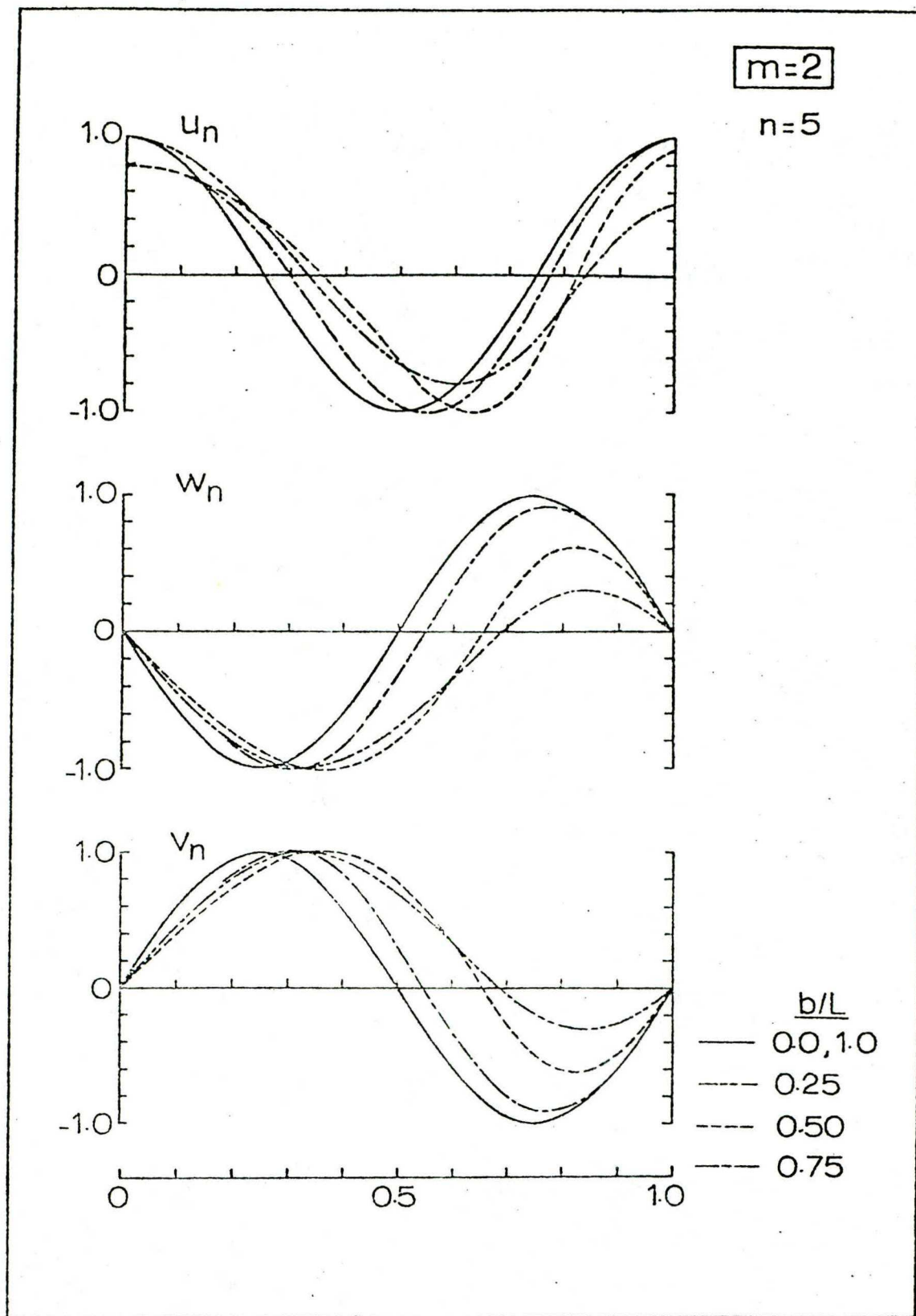


FIGURE 9

Eigenvectors of liquid-filled shells, as functions of liquid depth, b ; for $n = 5$, $m = 2$.

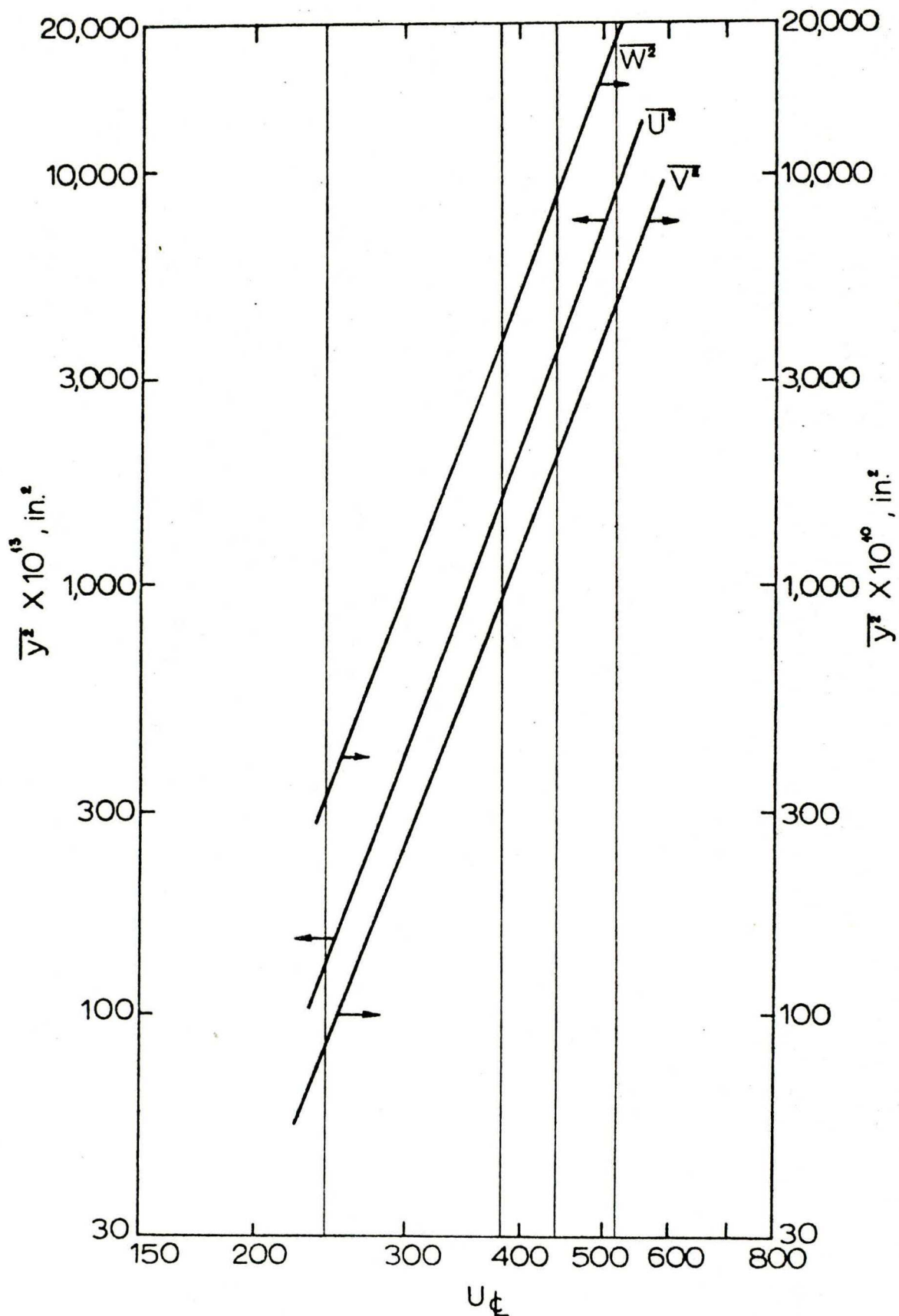


FIGURE 10 The mean square response of the radial, axial and circumferential displacements obtained by this theory (with $n = 2$ to $n = 12$) for the shell first studied by Clinch, ('total' response over whole frequency range).

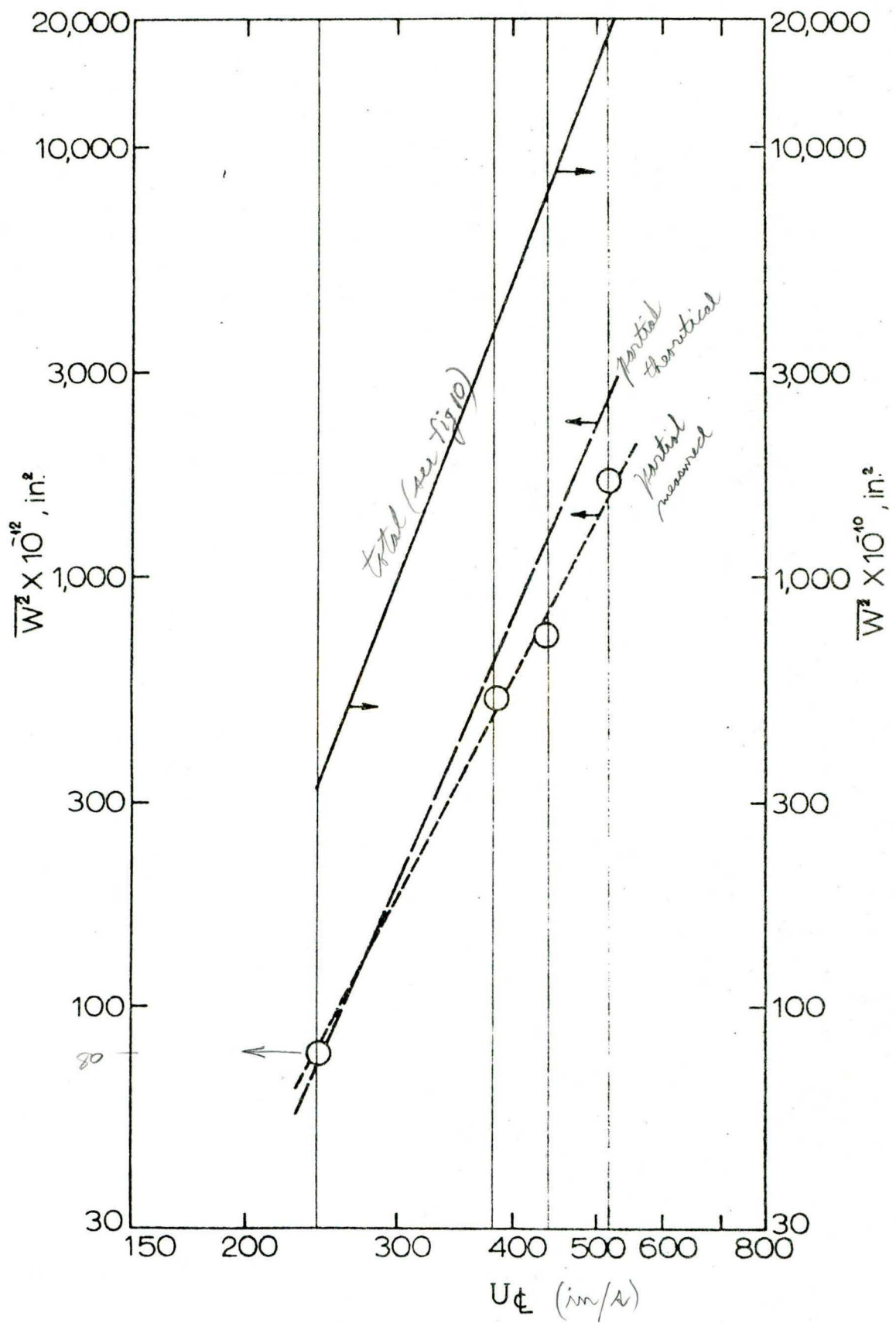


FIGURE 11 The mean square response of the radial displacement of a shell first studied by Clinch, as a function of the centerline velocity. -o--o- Clinch's experimental results for high-frequency response; - - - - theoretical results obtained by this theory (with $n = 2$ to $n = 12$) for high-frequency response (93 - 1,000 Hz); ——— 'total' response obtained by this theory (with $n = 2$ to $n = 12$).